generated by transplanting bone marrow cells infected with TPO retrovirus into lethally irradiated recipient mice [14–16] or by intraperitoneal injection of TPO cDNA in an adenovirus vector [17]. Myelofibrosis developed 10–12 weeks after BM transplantation (BMT) or adenovirus infection. On the other hand, transgenic mice overexpressing TPO using a liver-specific apolipoprotein E (Apo-E) promoter did not exhibit myelofibrosis or osteosclerosis [18]. These discrepancies in phenotype are not fully understood.

We have generated a mouse model to study the biological role of TPO in vivo by transgenic expression of the TPO cDNA using the mouse rearranged H chain promoter. These mice are expected to continuously secrete TPO from the bone marrow and spleen for the life of the animal. In contrast to the previous study using the Apo-E promoter, we show here that TPO Tg mice developed myelofibrosis and osteosclerosis.

2. Materials and methods

2.1. Mice

Murine TPO (mTPO) cDNA was amplified by polymerase chain reaction (PCR) from murine bone marrow cDNA using oligonucleotides primers specific for the murine TPO sequence: forward 5′-gac tct gcc gaa aga agc ac-3′ and reverse 5′-gct cga gaa gct gca gac gct cac t-3′, and subcloned into the pCR2.1-TOPO vector (Invitrogen, CA, USA). A 1.21-kb XhoI fragment containing the entire mTPO cDNA was cloned into the pEMVhp vector, which contains the mouse H chain enhancer (Eμ), the mouse rearranged H chain promoter, and the polyadenylation site from the rabbit β-globin gene [19]. The construct was isolated from vector sequences as a SacI/KpnI fragment and purified. Tg mice were produced by standard oocyte injection using BDF1 mice-derived fertilized eggs. Transgenic mice were identified by PCR using oligonucleotide primers specific for the mouse rearranged H chain promoter (forward primer; 5′-ggc tgg cgt gga aat att ct-3′) and the mTPO cDNA (reverse primer; 5′-gga cac tgc ccc tag aat gt-3′).

2.2. Hematologic blood parameters

Blood was collected from the retro-orbital plexus into heparin-coated microcapillary tubes (Terumo, Tokyo, Japan) which were reheparinized before use to avoid platelet clumping. Numbers of white blood cells (WBC) and platelets and hematocrit (Hct) values were determined immediately after collection with a Celltac (MEK-6158, Nihon Kohden, Tokyo, Japan). Differential counts of WBC were performed on Giemsa-stained slides, counting at least 100 cells.

2.3. Progenitor cell assays

Mononuclear cells from bone marrow and spleen were separated by Ficoll-Paque sedimentation. 1×10^5 isolated cells were cultured in 1 ml of a mixture containing Iscove's modified Dulbecco medium (IMDM) supplemented with fetal bovine serum (FBS, 30%, v/v) and methylcellulose (0.88%, w/v), and stimulated with a combination of recombinant growth factors including mouse stem cell factor (SCF, 20 ng/ml), mouse interleukin 3 (IL-3, 20 ng/ml), and human erythropoietin (Epo, 2 IU/ml). The growth of erythroid colony forming units (CFU-E)-derived colonies was stimulated with Epo alone (0.5 IU/ml). Cultures were incubated at 37 °C in humidified air with 5% CO_2, and scored with an inverted microscope on day 3 for CFU-E-derived colonies or on day 7 for granulocyte colony forming units (CFU-G)-, CFU-GM-, CFU-mix-, and BFU-E-derived colonies.

2.4. Histology

For histological evaluation, tissue samples (spleen, liver, and femur) were fixed in formalin, paraffin embedded, and cut for hematoxylin and eosin staining or Gomori silver staining according to standard protocols.

2.5. Cytokine quantification

TPO, Epo, transforming growth factors (TGF)-β1, and osteoprotegerin (OPG) levels in platelet-poor plasma (PPP) were determined with an enzyme-linked immunosorbent assay (ELISA) using the Quantikine Kits for each murine cytokine (R&D Systems, Minneapolis, MN, USA), according to the manufacturer's instructions. TGF-β1 was measured after acidification to activate latent forms into immunoreactive ones. For acidification, the procedure recommended by the supplier was followed without modifications. The sensitivity limits of the assays were 20 pg/ml for TPO, 18 pg/ml for Epo, 2.89 pg/ml for total TGF-β1, and 4.5 pg/ml for OPG.

2.6. Statistical analysis

The results are presented as mean ± S.D. Statistical significance was determined using the two-tailed Student's *t*-test.

3. Results

3.1. Generation of TPO overexpressing mice (Fig. 1A and B)

Tg mice were generated expressing full-length mTPO under the control of the mouse Ig enhancer and promoter (Fig. 1A). Transgenic founder mice were identified by transgene-specific amplification of genomic DNA using the polymerase chain reaction. Three transgenic lines were established, and the line in which platelet number was highest was analyzed further.

Mice were divided into two age groups (2–4 and 7–9 months of age) for convenience. Plasma levels of TPO were

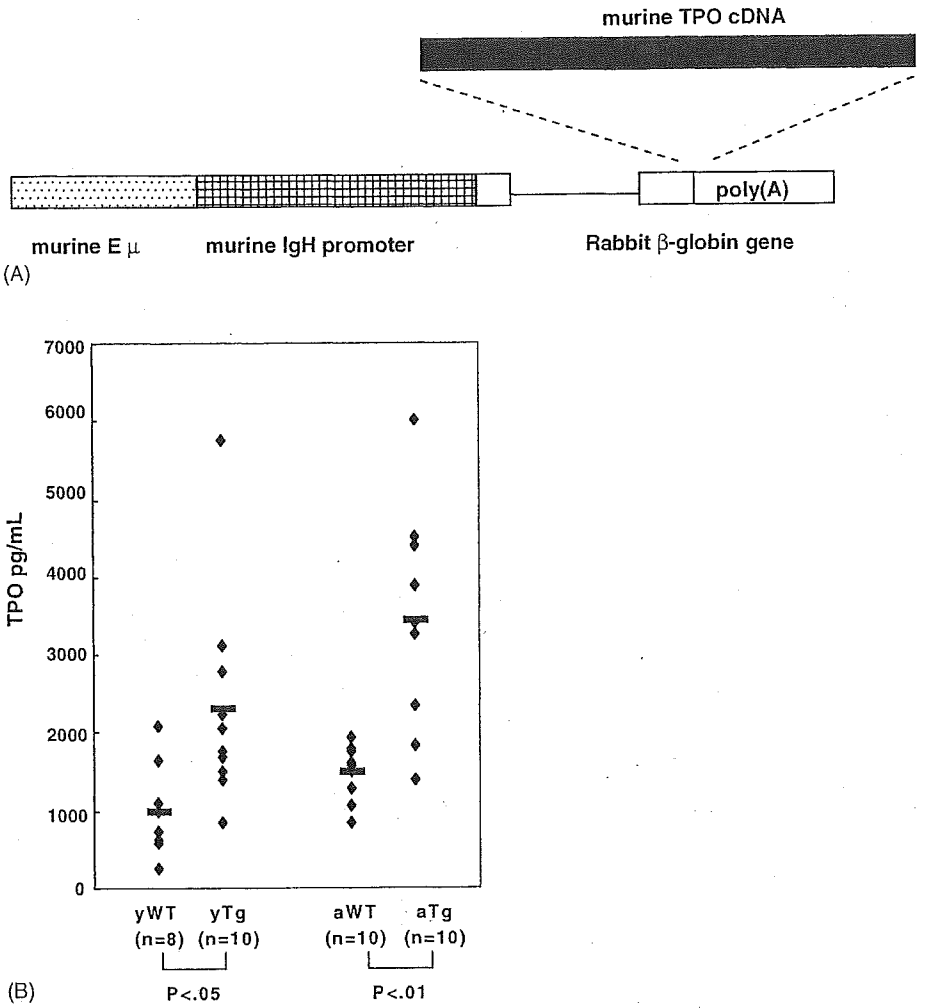

Fig. 1. Construction of Tg vector and plasma TPO levels in transgenic mice. (A) Schematic structure of transgene for the expression of murine TPO under the control of the mouse H chain promoter and intronic enhancer. (B) Plasma TPO levels in wild-type (WT) and TPO transgenic mice (Tg). Values were compared between two age groups, 2–4-month-old mice (young: y) and 7–9-month-old ones (adult: a); (–): mean value; *n*: number of mice.

measured by ELISA. Plasma TPO levels did not change during growth and were higher in TPO Tg mice than in wild-type mice. In adult mice, plasma TPO levels were 1.5 ± 0.3 ng/ml in wild-type littermates and 3.5 ± 1.5 ng/ml in TPO Tg mice ($p < 0.01$) (Fig. 1B).

3.2. Hematologic parameters in TPO overexpressing mice

Blood values in TPO Tg and wild-type littermates are shown in Fig. 2. The number of platelets rose with age in TPO Tg mice, and reached $211.5 \pm 82.3 \times 10^4/\mu l$ at 7–9 months, a value that was three times greater than that of normal ($69.3 \pm 10.1 \times 10^4/\mu l$) (Fig. 2A). The white blood cell count was also increased in TPO Tg mice (Fig. 2B). WBC differential counts revealed general proliferation of all cell types (including lymphocytes) corresponding to the increased number of WBC in TPO Tg mice. In particular, neutrophil counts were increased 2.8-fold compared to normal littermates (Fig. 2C). No morphologically immature or dysplastic cells were noted.

On the other hand, Hct values were decreased by approximately 10% in TPO Tg mice compared to age-matched normal littermates (Fig. 2D). As anemia was observed in TPO Tg mice, plasma Epo levels were next examined. In spite of the decreased Hct in TPO Tg mice, plasma Epo levels did not differ between wild-type and TPO Tg mice (Fig. 2E).

3.3. Bone marrow findings and frequency of hematopoietic progenitor cells (Table 1 and Fig. 3)

We next examined the number and morphology of bone marrow cells and the frequency of hematopoietic progenitor cells in TPO Tg mice. The total number of bone marrow mononuclear cells in TPO Tg mice was equivalent to that in normal littermates at 2–4 months of age, and then decreased with age (Table 1). We only obtained very few bone marrow

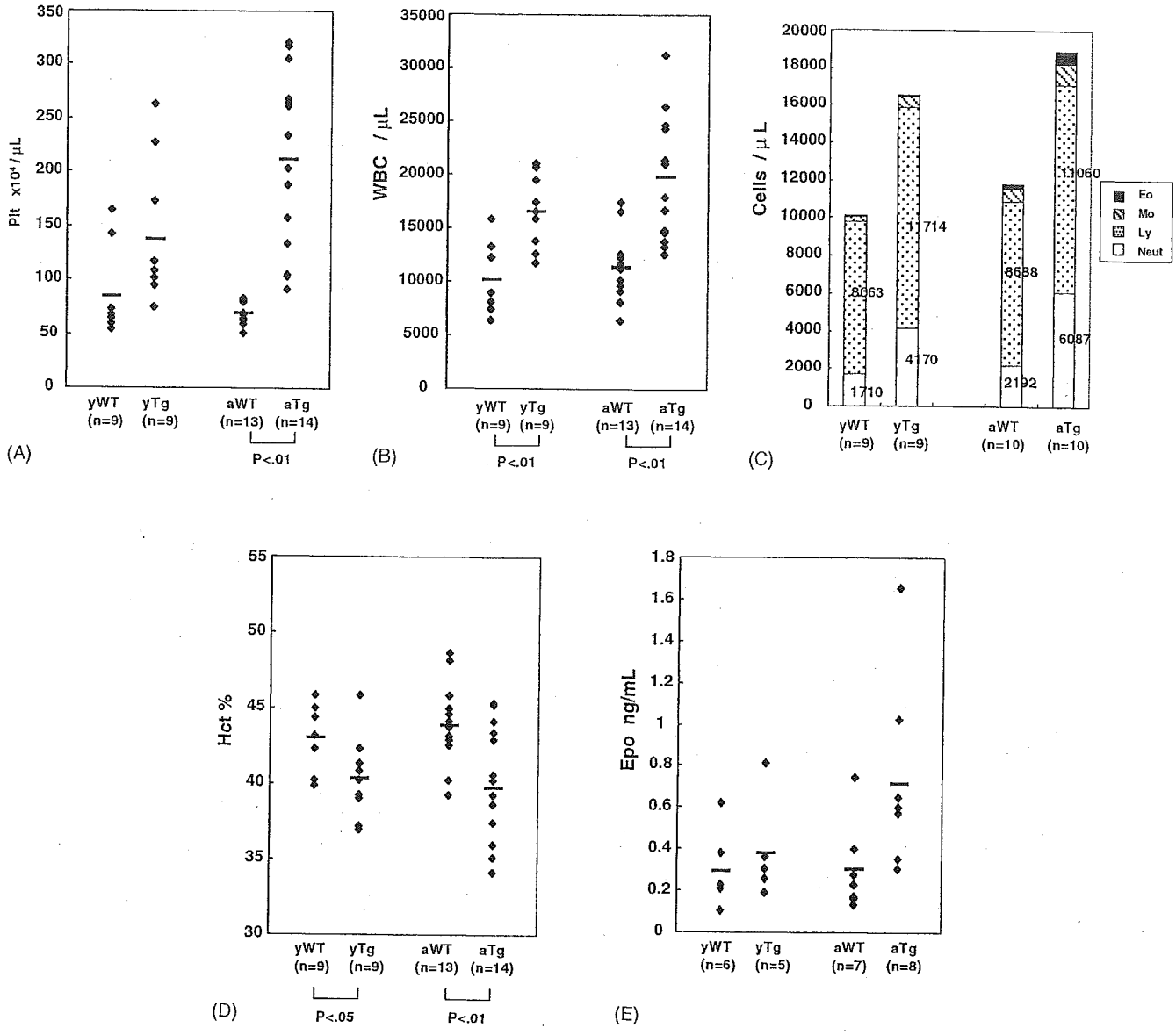

Fig. 2. Hematologic parameters and plasma Epo levels in age-matched wild-type and TPO Tg mice. Mice were arbitrarily divided into the same age groups used in Fig. 1B. (A) Platelet count × 10^4/μl. (B) White blood cell count (/μl). (C) Differential analysis of blood cells (/μl). Neut: neutrophils; Ly: lymphocytes; Mo: monocytes; and Eo: eosinophils. (D) Hematocrit (%). (E) Plasma Epo levels were measured by ELISA. Values in TPO Tg mice statistically different from those observed in the age-matched wild-type littermates are indicated by $p < 0.01$ and $p < 0.05$.

Table 1
Analysis of age-matched wild-type and TPO Tg mice

Items	2–4 months of age		7–9 months of age	
	WT	Tg	WT	Tg
BM				
MNCs/2 femora (×10^6)	9.3 ± 3.7	11.6 ± 3.1	16.8 ± 3.0	0.5 ± 0.1*
Spleen				
MNCs/spleen (×10^6)	16.2 ± 2.6	16.6 ± 4.5	15.6 ± 9.2	14.5 ± 6.1
Weight (mg)	87.2 ± 5.4	166.8 ± 51.2†	94.1 ± 13.0	315.4 ± 92.2†
Liver				
Weight (mg)	1106 ± 42	1502 ± 48†	1606 ± 221	1843 ± 174‡

Results are mean ± S.D. A total of 4 to 7 TPO Tg mice and 4 to 11 normal littermates were analyzed per each age group. Values in the TPO Tg mice statistically different from those in the corresponding wild-type animals are indicated by *$p < 0.0001$, †$p < 0.01$, and ‡$p < 0.05$.

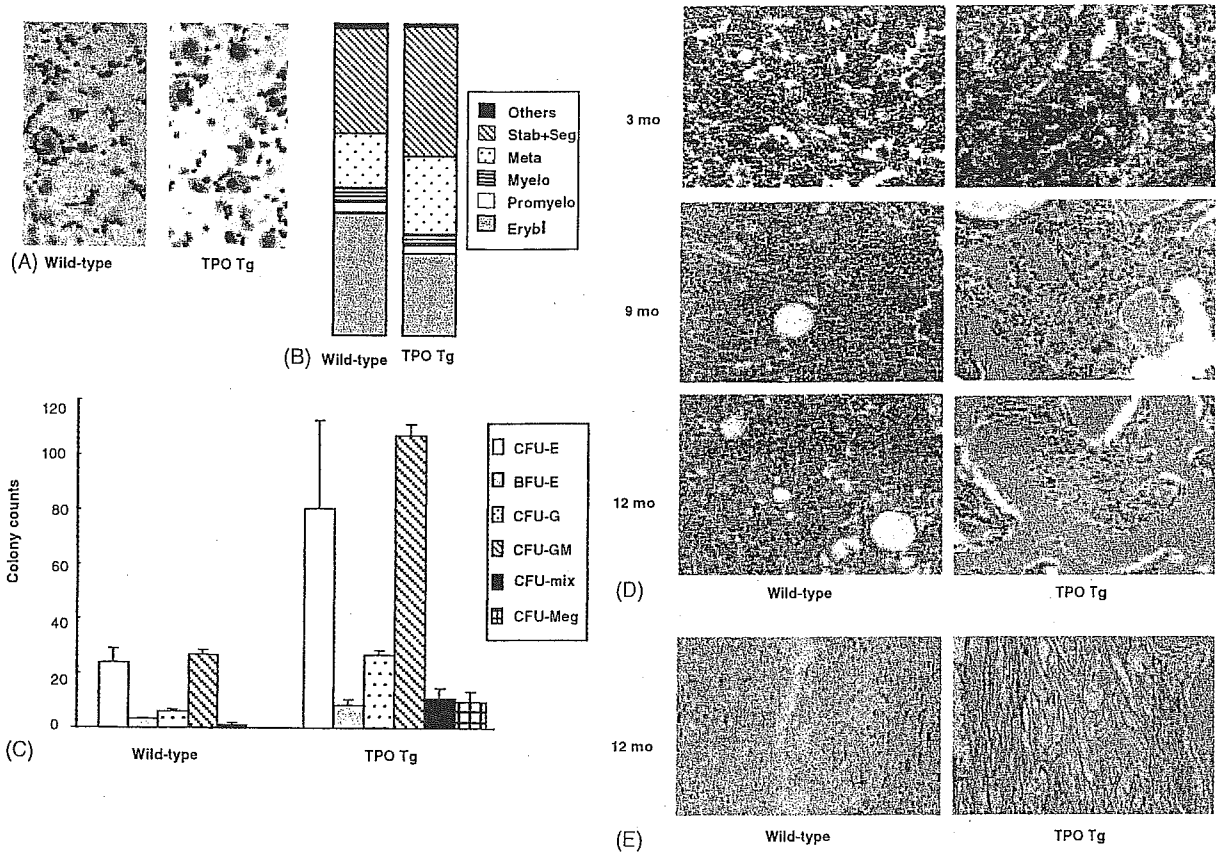

Fig. 3. Changes in bone marrow of TPO overexpressing mice. (A–C) Bone marrow cells were evaluated at 3 months of age in wild-type and TPO Tg mice. (A) Representative Giemsa staining of bone marrow smear. (B) Differential analysis of bone marrow cells. Stab; stab cells, Seg; segmented cells, Meta; metamyelocytes, Myelo; myelocytes, Promyelo; promyelocytes, Erybl; erythroblasts. (C) Frequency of hematopoietic colonies per 1×10^5 bone marrow mononuclear cells from 2- to 4-month-old wild-type and TPO Tg mice. Results are presented as the mean (±S.D.) of three independent experiments. (D–E) Histologic sections of bone marrow from progressively older (3, 9 and 12 months) wild-type (left pannels) and TPO Tg mice (right pannels). (D) Hematoxylin-eosin staining (×200). (E) Gomori silver staining (×200).

cells from adult (especially greater than 12-month-old) TPO Tg mice. Giemsa staining of bone marrow cells showed that the number of megakaryocytes was increased in TPO Tg mice (Fig. 3A), and differential counts revealed a reduced proportion of erythroblasts in TPO Tg mice (Fig. 3B). Considering that there was no difference in the number of mononuclear cells between normal littermates and TPO Tg mice at this age (Table 1), erythroblasts in TPO Tg bone marrow were decreased in absolute number.

The frequency of hematopoietic progenitor cells was assessed by colony formation from 2- to 4-month-old mice (Fig. 3C). The number of CFU-Meg was 5 ± 4.5 in 1×10^5 bone marrow mononuclear cells from TPO Tg mice, although no megakaryocyte colonies formed from wild-type mice under the same conditions. The numbers of CFU-mix, CFU-GM, and CFU-G were increased by 10.4-, 3.5-, and 3.5-fold in bone marrow cells from TPO Tg mice compared to normal littermates. In spite of the anemia observed in TPO Tg mice, the number of CFU-E or BFU-E was not decreased but rather increased by 2.4-fold in bone marrow cells from TPO Tg mice compared to wild-type mice.

3.4. Development of myelofibrosis and osteosclerosis in TPO overexpressing mice (Fig. 3D and E)

Hematoxylin and eosin examination of bone marrow sections from 3-month-old TPO Tg mice showed an increased number of megakaryocytes, but no abnormalities of bone marrow architecture including fibrotic change or altered bone formation (Fig. 3D). Myelofibrosis and osteomyelosclerosis developed in the marrow of TPO Tg mice with age. Nine-month-old TPO Tg mice showed a reduction in space for hematopoietic cells and increased bone trabeculae and intercellular matrix. In 12-month-old TPO Tg mice, the bone trabeculae and intercellular matrix became massive. Gomori silver staining showed an accumulation of fibers in the intercellular space of the marrow from adult TPO Tg mice (Fig. 3E).

3.5. Increased extramedullary hematopoiesis and fibrosis in the spleen (Table 1 and Fig. 4)

TPO Tg mice displayed marked splemomegaly (Fig. 4A), with splenic weight about two to three times wild-type mice

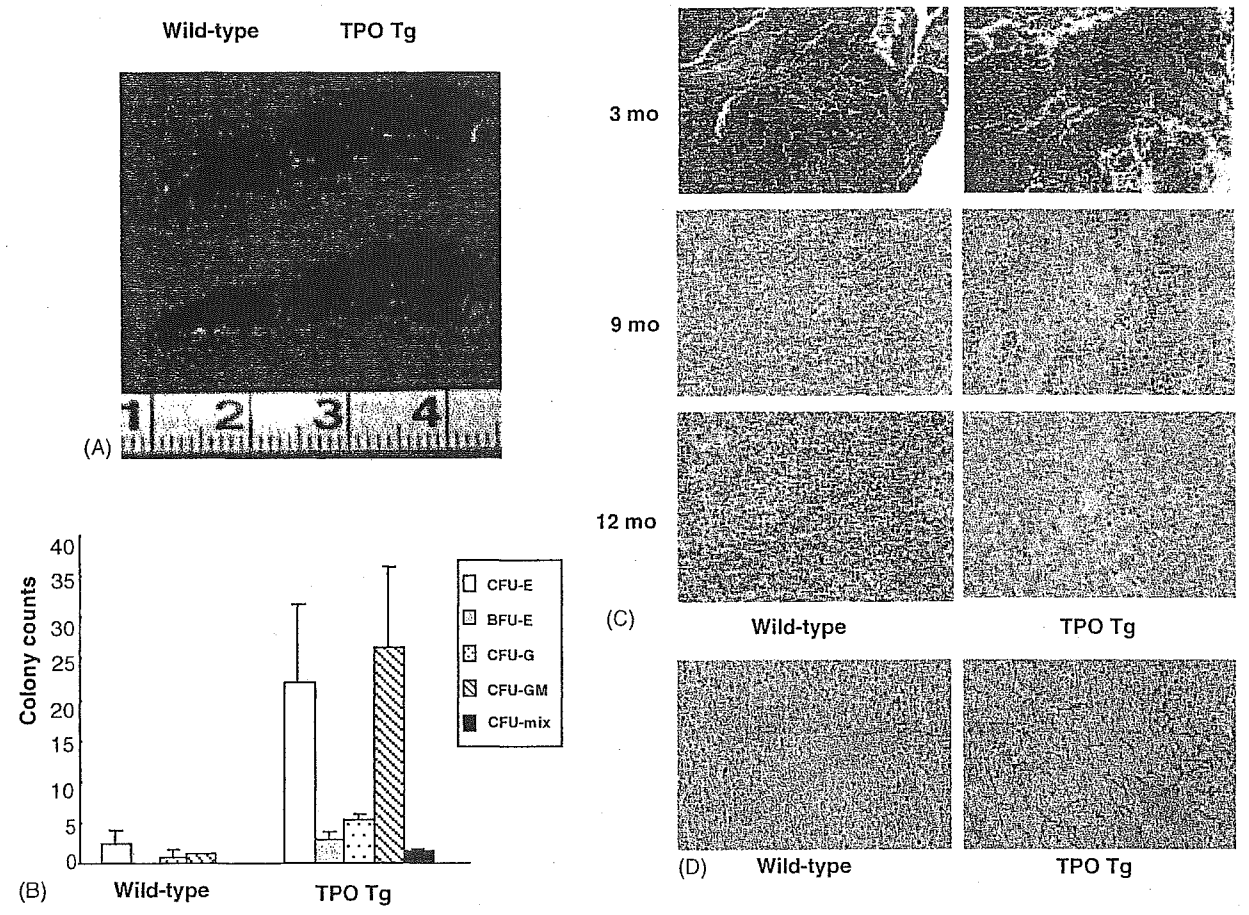

Fig. 4. Extramedullary hematopoiesis and fibrotic change in spleens of TPO overexpressing mice. (A) Macroscopic appearance of spleens from 9-month-old TPO Tg mice (right) and from corresponding wild-type mice (left). (B) Frequency of hematopoietic colonies per 1×10^5 spleen mononuclear cells from 2- to 4-month-old wild-type and TPO Tg mice. Results are presented as the mean (±S.D.) of three independent experiments. (C–D) Histologic sections of spleen from progressively older (3, 9 and 12 months) wild-type and TPO Tg mice. (C) Hematoxylin-eosin staining (×200). (D) Gomori silver staining (×200).

(Table 1). Despite the enlarged splenic size and weight in TPO Tg mice, there was no difference in the total number of mononuclear cells between TPO Tg and wild-type mice (Table 1). Colony-forming cells were rarely observed in spleens from wild-type mice. On the other hand, the numbers of CFU-GM, CFU-Meg, CFU-mix, and BFU-E in spleen cells from TPO Tg mice were much greater than those from normal littermates respectively (Fig. 4B).

With age, expanded fibrotic tissue surrounding islands of hematopoiesis and megakaryocytes was observed in spleens from TPO Tg mice (Fig. 4C). An accumulation of reticulin fibers was also documented in TPO Tg mice (Fig. 4D).

As for the liver, there were no histological abnormalities in TPO Tg mice, even in 12-month-old animals. However, the liver weight in TPO Tg mice was greater than that in wild-type mice throughout growth (Table 1).

3.6. Plasma levels of TGF-β1 and OPG (Fig. 5)

To clarify the basis for the fibrosis and osteosclerosis observed in TPO Tg mice, we measured the levels of plasma TGF-β1 and OPG. Compared with normal littermates, total TGF-β1 was three- to four-fold higher in plasma from TPO Tg mice (43 ± 23 versus 148 ± 89 ng/ml at 2–4 months, 43 ± 16 versus 178 ± 150 ng/ml at 7–9 months, respectively) (Fig. 5A). Plasma OPG levels did not differ between young wild-type and TPO Tg mice (2.7 ± 0.2 ng/ml in WT and 2.3 ± 0.1 ng/ml in Tg). Plasma OPG levels were not changed with age in wild-type mice. On the other hand, plasma OPG levels rose with age in TPO Tg mice. Then in adult mice, plasma OPG levels were higher in TPO Tg mice (3.8 ± 0.3 ng/ml) than in wild-type mice (2.2 ± 0.1 ng/ml) ($p < 0.01$) (Fig. 5B).

4. Discussion

We have shown that IgH promoter-derived murine TPO cDNA overexpression in vivo produces a 2.3-fold elevation in TPO protein compared with wild-type mice, for at least 9 months (Fig. 1B). The elevated TPO levels in TPO Tg mice caused an increase in the number of CFU-Meg and megakaryocytes in bone marrow and of platelets in peripheral blood (Figs. 2A, 3A, C and D). In addition to the effects

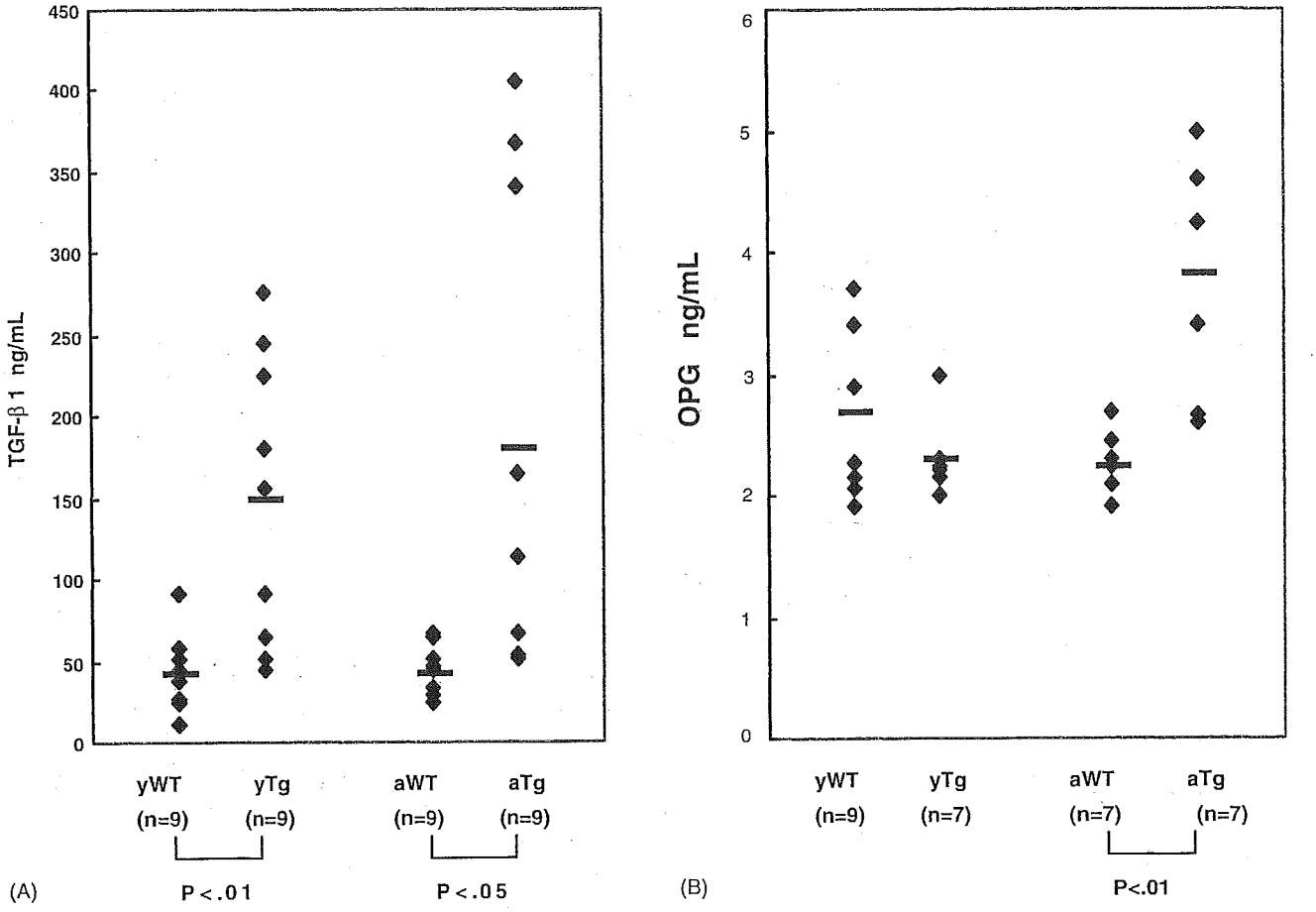

Fig. 5. Plasma TGF-β1 and OPG levels. (A) Total TGF-β1 and (B) OPG levels in plasma. Levels were determined by ELISA. TGF-β1 was measured after acidification of the samples as described in Section 2. The age groups of mice were the same as those used in Fig. 1B. Values in TPO Tg mice statistically different from those observed in the age-matched wild-type littermates are indicated by $p < 0.01$ and $p < 0.05$.

on megakaryocytopoiesis, the number of CFU-mix, CFU-GM, and CFU-G in bone marrow was increased in TPO Tg mice (Fig. 3C). This means that TPO increases the number of hematopoietic progenitor cells in vivo, not only progenitors committed to the megakaryocyte lineage. TPO acts additively or synergistically with IL-3 and stem cell factor to promote the growth of primitive stem cells [20–22], as well as progenitor cells giving rise to BFU-E, CFU-GM, and CFU-mix [23,24]. Both erythroid and myeloid progenitor cells were conspicuously decreased in TPO or TPO receptor deficient mice [8,9]. Consistent with this, in TPO Tg mice the number of neutrophils in peripheral blood was increased 2.8-fold (Fig. 2C), and the number of myeloid cells in bone marrow was increased compared to wild-type mice (Fig. 3B).

As for erythrocytes, TPO Tg mice showed anemia. The Hct value was slightly but significantly decreased in TPO Tg mice compared with wild-type mice (Fig. 2D). The number of erythroblasts in bone marrow from TPO Tg mice was also decreased relative to that from wild-type mice (Fig. 3B). On the other hand, the number of CFU-E and BFU-E were increased 2.4-fold in TPO Tg mice compared with wild-type mice (Fig. 3C). As there was no difference in the number of mononuclear cells in bone marrow between young TPO Tg and wild-type mice (Table 1), the total numbers of erythroid progenitor cells per animal was thought to be increased in TPO Tg mice. Zhou et al. already reported anemia and increased number of CFU-E in TPO Tg mice, generated by a liver-specific Apo-E promoter [18]. This means that the differentiation from erythroid lineage-progenitor cells to erythroblasts was disrupted by overexpression of TPO in bone marrow. We then measured Epo levels in vivo, as the CFU-E or BFU-E assay is performed in the presence of Epo in vitro. As shown in Fig. 2E, there was no difference in plasma Epo levels between TPO Tg and wild-type mice. One possibility to explain the discrepancy between the increased number of CFU-E in vitro and the decreased number of erythroblasts in bone marrow and the decreased Hct value in peripheral blood may be that a higher amount of TPO influences the fate of progenitor cells capable of differentiating to erythroid cells in vivo. If this is the case, the progenitor cells for the erythrocyte lineage are also able to differentiate into megakaryocytes in the presence of TPO, while the fate of progenitor cells for neutrophils or monocytes is not affected by the presence of TPO.

In our TPO Tg mice, TPO might act on hematopoietic stem cells and augment the number of progenitor cells, resulting in increased numbers of colony-forming cells in vitro. TPO might also act on common progenitor cells for megakaryocytes and erythrocytes and drive these bipotential progenitors to differentiate to the megakaryocyte lineage, resulting in decreased differentiation into erythroid lineage cells in vivo.

TPO Tg mice, with expression under the control of the IgH promoter, exhibited myelofibrosis and osteosclerosis 9 months after birth (Fig. 3D and E). This is consistent with other reports in which bone marrow cells were retrovirally transduced with TPO cDNA and then transplanted into irradiated recipients [14–16] or in which mice were transfected with adenovirus containing TPO [17]. Transgenic mice, in which TPO cDNA was expressed under the control of the Apo-E promoter, did not develop myelofibrosis or osteosclerosis [18]. As hematopoietic progenitor cells are also the target of transfection with retrovirus containing human TPO cDNA in the BMT model, the nature of the retrovirally transfected cells might be important for developing myelofibrosis. Only overproduction of TPO by adenoviral transfection [17] or in transgenic mice described here induced myelofibrosis and osteosclerosis in mice. This means that exposure to high amounts of TPO is enough to develop myelofibrosis and osteosclerosis in vivo. However, the period for developing myelofibrosis and osteosclerosis seems to be different among the models. Adenovirus transfected mice develop myelofibrosis within 80 days [17]. On the other hand, our TPO Tg mice did not develop myelofibrosis within 3 months, but developed myelofibrosis and osteosclerosis 9 months after birth (Fig. 3D). This may be accounted for by different plasma TPO levels between the two models. Plasma TPO levels are about 10-fold higher in the virally transfected model than in control mice [17], and TPO Tg mice showed only a two to three-fold increase in plasma TPO levels compared to wild-type mice (Fig. 1B). Exposure to very high amounts of TPO may lead to the development of myelofibrosis and osteosclerosis within a relatively short period, while exposure to a relatively small amount of TPO may take more time to induce and establish the same histological changes. This may explain the phenomenon that TPO Tg mice driven by the Apo-E promoter do not develop myelofibrosis and osteosclerosis [18]. Serum TPO levels were comparable between TPO Tg mice driven by the Apo-E promoter and IgH promoter. Local TPO levels in bone marrow should be different though, with TPO Tg mice expressing under the control of the IgH promoter having much higher TPO levels in bone marrow relative to TPO Tg mice expressing under the control of the Apo-E promoter. The pathogenesis of myelofibrosis and osteosclerosis in TPO overexpressing mice was thought to be due to elevated cytokines released from the increased number of megakaryocytes or stromal cells. Such cytokines could directly stimulate the fibrogenic and osteogenic response [16]. We measured plasma levels of TGF-β1 and OPG, and showed that these cytokines were elevated in TPO Tg mice compared with wild-type littermates (Fig. 5). TGF-β1 is a protein that binds to proteoglycans in the extracellular matrix, and has broad effects on many cell types, including fibroblasts and osteoblasts [25]. It, thus, remains likely that an expanded population of megakaryocytes in BM from TPO Tg mice leads to locally increased secretion of TGF-β1 that stimulates surrounding fibroblasts to proliferate and produce collagen, resulting in the observed myelofibrosis. In fact, mice engrafted with TGF-β1-deficient-TPO-overexpressing BM cells did not develop myelofibrosis [26].

The involvement of OPG in osteosclerosis has already been reported. Mice engrafted with OPG-deficient-TPO-overexpressing BM cells developed myelofibrosis, but did not develop osteosclerosis [27]. Osteoclast differentiation and activation is facilitated by the interaction between RANK (receptor activator of NF-kB) and RANK ligand (RANKL (also known as OPGL)) [28–31]. OPG is a decoy receptor of RANKL and interferes with RANK-RANKL binding, resulting in impaired bone resorption [32]. OPG is mainly secreted by bone marrow stromal cells and osteoblasts [32]. OPG-deficient host mice engrafted with wild-type TPO-overexpressing BM cells did not develop osteosclerosis, and plasma OPG levels were also elevated in wild-type host mice engrafted with TPO virus-infected BM from OPG-deficient donors. Thus, the main source of OPG observed in TPO overexpressing mice was reported to be stromal cells in the host, not transplanted bone marrow cells [27]. Megakaryocytes can also produce OPG [33]. OPG secreted from both megakaryocytes and stromal cells by stimulation from high amounts of TPO might lead to the development of bone sclerosis in TPO Tg mice.

Acknowledgments

We thank M. Sato and M. Ito for their excellent technical assistance. This work was supported in part by a Grant from the Japan Leukemia Foundation and Grants-in-Aid for Scientific Research (numbers 13218096, 15390302) from the Ministry of Education, Culture, Sports, Science, and Technology in Japan.

H. Kakumitsu contributed to the concept and design, interpreted and analyzed the data, provided drafting of the article, provided study materials, supplied the statistical analysis, collected and assembled the data. K. Kamezaki interpreted and analyzed the data, provided critical revisions and important intellectual content. K. Shimoda contributed to the concept and design, provided critical revisions and important intellectual content, obtained a funding source, and gave final approval. K. Karube and K. Oshima contributed to the pathological experiments. T. Haro, A. Numata, K. Shide, and T. Matsuda provided critical revisions and important intellectual content. M. Harada provided critical revisions and important intellectual content, and obtained a funding source.

References

[1] Kaushansky K, Lok S, Holly RD, et al. Promotion of megakaryocyte progenitor expansion and differentiation by the c-Mpl ligand thrombopoietin. Nature 1994;369:568–71.

[2] Lok S, Kaushansky K, Holly RD, et al. Cloning and expression of murine thrombopoietin cDNA and stimulation of platelet production in vivo. Nature 1994;369:565–8.

[3] Wendling F, Maraskovsky E, Debili N, et al. cMpl ligand is a humoral regulator of megakaryocytopoiesis. Nature 1994;369:571–4.

[4] Bartley TD, Bogenberger J, Hunt P, et al. Identification and cloning of a megakaryocyte growth and development factor that is a ligand for the cytokine receptor Mpl. Cell 1994;77:1117–24.

[5] Chang MS, McNinch J, Basu R, et al. Cloning and characterization of the human megakaryocyte growth and development factor (MGDF) gene. J Biol Chem 1995;270:511–4.

[6] de Sauvage FJ, Carver-Moore K, Luoh SM, et al. Physiological regulation of early and late stages of megakaryocytopoiesis by thrombopoietin. J Exp Med 1996;183:651–6.

[7] Gurney AL, Carver-Moore K, de Sauvage FJ, et al. Thrombocytopenia in c-mpl-deficient mice. Science 1994;265:1445–7.

[8] Carver-Moore K, Broxmeyer HE, Luoh SM, et al. Low levels of erythroid and myeloid progenitors in thrombopoietin-and c-mpl-deficient mice. Blood 1996;88:803–8.

[9] Alexander WS, Roberts AW, Nicola NA, et al. Deficiencies in progenitor cells of multiple hematopoietic lineages and defective megakaryocytopoiesis in mice lacking the thrombopoietic receptor c-Mpl. Blood 1996;87:2162–70.

[10] Solar GP, Kerr WG, Zeigler FC, et al. Role of c-mpl in early hematopoiesis. Blood 1998;92:4–10.

[11] Gainsford T, Roberts AW, Kimura S, et al. Cytokine production and function in c-mpl-deficient mice: no physiologic role for interleukin-3 in residual megakaryocyte and platelet production. Blood 1998;91:2745–52.

[12] Kaushansky K, Fox N, Lin NL, et al. Lineage-specific growth factors can compensate for stem and progenitor cell deficiencies at the postprogenitor cell level: an analysis of doubly TPO- and G-CSF receptor-deficient mice. Blood 2002;99:3573–8.

[13] Ramsfjell V, Borge OJ, Veiby OP, et al. Thrombopoietin, but not erythropoietin, directly stimulates multilineage growth of primitive murine bone marrow progenitor cells in synergy with early acting cytokines: distinct interactions with the ligands for c-kit and FLT3. Blood 1996;88:4481–92.

[14] Villeval JL, Cohen-Solal K, Tulliez M, et al. High thrombopoietin production by hematopoietic cells induces a fatal myeloproliferative syndrome in mice. Blood 1997;90:4369–83.

[15] Yan XQ, Lacey D, Hill D, et al. A model of myelofibrosis and osteosclerosis in mice induced by overexpressing thrombopoietin (mpl ligand): reversal of disease by bone marrow transplantation. Blood 1996;88:402–9.

[16] Yan XQ, Lacey D, Fletcher F, et al. Chronic exposure to retroviral vector encoded MGDF (mpl-ligand) induces lineage-specific growth and differentiation of megakaryocytes in mice. Blood 1995;86:4025–33.

[17] Frey BM, Rafii S, Teterson M, et al. Adenovector-mediated expression of human thrombopoietin cDNA in immune-compromised mice: insights into the pathophysiology of osteomyelofibrosis. J Immunol 1998;160:691–9.

[18] Zhou W, Toombs CF, Zou T, et al. Transgenic mice overexpressing human c-mpl ligand exhibit chronic thrombocytosis and display enhanced recovery from 5-fluorouracil or antiplatelet serum treatment. Blood 1997;89:1551–9.

[19] Yasui T, Muraoka M, Takaoka-Shichijo Y, et al. Dissection of B cell differentiation during primary immune responses in mice with altered CD40 signals. Int Immunol 2002;14:319–29.

[20] Sitnicka E, Lin N, Priestley GV, et al. The effect of thrombopoietin on the proliferation and differentiation of murine hematopoietic stem cells. Blood 1996;87:4998–5005.

[21] Ku H, Yonemura Y, Kaushansky K, et al. Thrombopoietin, the ligand for the Mpl receptor, synergizes with steel factor and other early acting cytokines in supporting proliferation of primitive hematopoietic progenitors of mice. Blood 1996;87:4544–51.

[22] Young JC, Bruno E, Luens KM, et al. Thrombopoietin stimulates megakaryocytopoiesis, myelopoiesis, and expansion of CD34+ progenitor cells from single CD34+Thy-1+Lin-primitive progenitor cells. Blood 1996;88:1619–31.

[23] Kobayashi M, Laver JH, Kato T, et al. Recombinant human thrombopoietin (Mpl ligand) enhances proliferation of erythroid progenitors. Blood 1995;86:2494–9.

[24] Papayannopoulou T, Brice M, Farrer D, et al. Insights into the cellular mechanisms of erythropoietin-thrombopoietin synergy. Exp Hematol 1996;24:660–9.

[25] Roberts AB, Sporn MB. Physiological actions and clinical applications of transforming growth factor-beta (TGF-beta). Growth Factors 1993;8:1–9.

[26] Chagraoui H, Komura E, Tulliez M, et al. Prominent role of TGF-beta 1 in thrombopoietin-induced myelofibrosis in mice. Blood 2002;100:3495–503.

[27] Chagraoui H, Tulliez M, Smayra T, et al. Stimulation of osteoprotegerin production is responsible for osteosclerosis in mice overexpressing TPO. Blood 2003;101:2983–9.

[28] Li J, Sarosi I, Yan XQ, et al. RANK is the intrinsic hematopoietic cell surface receptor that controls osteoclastogenesis and regulation of bone mass and calcium metabolism. Proc Natl Acad Sci USA 2000;97:1566–71.

[29] Lacey DL, Timms E, Tan HL, et al. Osteoprotegerin ligand is a cytokine that regulates osteoclast differentiation and activation. Cell 1998;93:165–76.

[30] Kong YY, Yoshida H, Sarosi I, et al. OPGL is a key regulator of osteoclastogenesis, lymphocyte development and lymph-node organogenesis. Nature 1999;397:315–23.

[31] Dougall WC, Glaccum M, Charrier K, et al. RANK is essential for osteoclast and lymph node development. Genes Dev 1999;13:2412–24.

[32] Simonet WS, Lacey DL, Dunstan CR, et al. Osteoprotegerin: a novel secreted protein involved in the regulation of bone density. Cell 1997;89:309–19.

[33] Chagraoui H, Sabri S, Capron C, et al. Expression of osteoprotegerin mRNA and protein in murine megakaryocytes. Exp Hematol 2003;31:1081–8.

Available online at www.sciencedirect.com
SCIENCE DIRECT
Biochimica et Biophysica Acta 1733 (2005) 101–110
BIOCHIMICA ET BIOPHYSICA ACTA BBA
http://www.elsevier.com/locate/bba

Regular paper

Sphingosine kinase 1 is involved in dibutyryl cyclic AMP-induced granulocytic differentiation through the upregulation of extracellular signal-regulated kinase, but not p38 MAP kinase, in HL60 cells

Masahiro Koda[a], Takashi Murate[b], Shulin Wang[a,1], Kenji Ohguchi[c], Sayaka Sobue[b], Mika Ikeda[c], Keiko Tamiya-Koizumi[d], Yasuyuki Igarashi[c], Yoshinori Nozawa[e], Yoshiko Banno[a,*]

[a]*Department of Cell Signaling, Gifu University Graduate School of Medicine, Yanagido 1-1, Gifu 501-1194, Japan*
[b]*Nagoya University School of Health Sciences, Nagoya, Japan*
[c]*Department of Biomembrane and Biofunctional Chemistry, Graduate School of Pharmaceutical Sciences, Hokkaido University, Sapporo, Japan*
[d]*Center for Neural Disease and Cancer, Nagoya University Graduate School of Medicine, Nagoya, Japan*
[e]*Gifu International Institute of Biotechnology, Kakamigahara, Japan*

Received 23 March 2004; received in revised form 19 October 2004; accepted 16 December 2004
Available online 5 January 2005

Abstract

The role of sphingosine kinase (SPHK) in the dibutyryl cyclic AMP (dbcAMP)-induced granulocytic differentiation of HL60 cells was investigated. During differentiation, SPHK activity was increased, as were mRNA and protein levels of SPHK1, but not of SPHK2. Pretreatment of HL60 cells with *N,N*-dimethylsphingosine (DMS), a potent SPHK inhibitor, completely blocked dbcAMP-induced differentiation. The phosphorylation of mitogen-activated protein kinases (MAPKs), extracellular signal-regulated kinase 1/2 (ERK1/2), and p38 MAPK was also increased during dbcAMP-induced differentiation. Pretreatment of HL60 cells with the MEK inhibitor, U0126, but not the p38 MAPK inhibitor, SB203580, completely suppressed dbcAMP-induced ERK1/2 activation and granulocytic differentiation, but did not affect the increase in SPHK activity. DMS inhibited dbcAMP-induced ERK1/2 activation, but had little effect on p38 MAPK activation. DMS had no effect on the dbcAMP-induced membrane translocation of protein kinase C (PKC) isozymes, and PKC inhibitors had no significant effect on ERK activation. The overexpression of wild-type SPHK1, but not dominant negative SPHK1, resulted in high basal levels of ERK1/2 phosphorylation and stimulated granulocytic differentiation in HL60 cells. These data show that SPHK1 participates in the dbcAMP-induced differentiation of HL60 cells by activating the MEK/ERK pathway.

Keywords: Sphingosine kinase; ERK; p38 MAP kinase; Differentiation; HL60 cell

1. Introduction

Sphingosine-1-phosphate (S1P), produced from sphingosine by sphingosine kinase (SPHK), is a bioactive sphingolipid metabolite that regulates diverse cellular responses, such as cell proliferation, differentiation, and apoptosis, acting both intra- and extracellularly [1–5]. Increases in S1P levels are implicated in the activation of the transcription factor, Ap-1, stimulation of the MAPK pathway, activation of phospholipase D, and increased expression of adhesion molecules [6–8]. Interest in S1P has focused on two distinct cellular actions of this lipid, namely as an extracellular

Abbreviations: SPHK, sphingosine kinase; S1P, sphingosine-1-phosphate; DMS, *N*, *N*-dimethylsphingosine; dbcAMP, dibutyryl cyclic AMP; NBT, nitroblue tetrazolium; fMLP, *N*-formyl-methionyl-leucyl-phenylalanine; ERK, extracellular regulating protein kinase; MAPK, mitogen activated protein kinase; PKC, protein kinase C; PTX, pertussis toxin

* Corresponding author. Tel./fax: +81 58 230 6202.
E-mail address: banno@cc.gifu-u.ac.jp (Y. Banno).
[1] Present address: Department of Medicine, University of Pennsylvania School of Medicine, Philadelphia, PA 19104, USA.

1388-1981/$ - see front matter © 2004 Elsevier B.V. All rights reserved.
doi:10.1016/j.bbalip.2004.12.006

ligand activating specific G protein-coupled membrane receptors (the S1P receptor family) and as an intracellular second messenger [1,2,9]. SPHK activation is mediated by various receptors, such as G protein-coupled receptors, growth factor receptors, Fc receptors, and tumor necrosis factor-α receptors [10–12]. The inhibition of SPHK markedly reduces or prevents certain cellular events, such as the activation of MAP kinases, stimulation of DNA synthesis, Ca^{2+} mobilization, and vesicular trafficking [13,14]. SPHK is therefore considered to play an important role in various cell functions, but the precise mechanisms by which it contributes to these physiological events remain to be elucidated.

Two isozymes of mammalian SPHK, SPHK1 and SPHK2, have been cloned and characterized [15,16]. SPHK1 and SPHK2 have different properties, tissue distributions, and temporal expression patterns, suggesting that they have different cellular functions and may be regulated differently [2,15,16]. In addition, two SPHK1 subtypes, SPHK1a and SPHK1b, have been cloned in the mouse [15]. SPHK activity is greatly increased during the nerve growth factor (NGF)-induced differentiation of pheochromocytoma PC12 cells [4], suggesting that it may play an important role in this differentiation process. A recent study demonstrated that SPHK activity is increased in differentiated F9 embryonal carcinoma cells, and that differentiation is accelerated by the overexpression of SPHK1 [5]. In contrast, our previous study demonstrated that SPHK1 had a negative regulatory effect on hepatocyte differentiation [17]. We have found that SPHK exists in multiple forms in human platelets, and that SPHK1 is expressed at high levels in the brain, kidney, vessel endothelial cells, megakaryocytes, and platelets [18–20]. We also demonstrated that SPHK1 protein levels are higher in 4β-phorbol 12-myristate 13 acetate (PMA)-induced differentiated HEL human leukemia cells than in the undifferentiated cells [19], suggesting that SPHK1 plays a role in human megakaryocytic differentiation. Together, these results suggest that SPHK plays important regulatory roles in cell differentiation, although the mechanisms involved have yet to be determined.

The human myeloid HL60 cell line can be induced to differentiate either into mature granulocytes by treatment with dibutyryl cyclic AMP (dbcAMP), dimethyl sulfoxide, or retinoic acid, or into monocytes by treatment with PMA [21], and treatment of HL60 cells with the differentiation-inducing agent, vitamin D3, induces SPHK activation, resulting in an increase in S1P levels [22]. Since we had previously studied signal transduction during the dbcAMP-induced granurocytic differentiation of HL60 cells [23,24], it was therefore of interest to determine the role(s) of SPHK in this process.

There is evidence that the MAP kinase signaling pathway is involved in the monocytic and granulocytic differentiation of leukemia cell lines. The MEK/ERK pathway is required for the differentiation of leukemia cells into monocytes and granulocytes [25,26], while the p38 MAPK pathway has a negative regulatory effect on monocytic differentiation, but promotes erythroid differentiation [27–29]. The link between SPHK and ERK is not clearly understood. Recently, it has been shown that, in platelet-derived growth factor (PDGF) and vascular endothelial growth factor (VEGF) signaling, ERK activation is dependent on SPHK [30,31].

In order to gain an insight into the mechanisms underlying the involvement of SPHK in differentiation process and the link between SPHK and MAPKs, we examined changes in SPHK activity, in SPHK1 and SPHK2 mRNA and protein levels, and in MAPK activity during the dbcAMP-induced granulocytic differentiation of HL60 cells and found that SPHK activity and the phosphorylation of MAPKs, ERK, and p38 MAPK were increased during this process, and that the phosphorylation of ERK1/2, but not of p38 MAPK, was upregulated by SPHK1.

2. Materials and methods

2.1. Materials

dbcAMP, nitroblue tetrazolium (NBT), PMA, and *N*-formyl-methionyl-leucyl-phenylalanine (fMLP) were purchased from Sigma Chemical Co (St. Louis, MO, USA). D-Erythro-sphingosine and *N*,*N*-dimethylsphingosine (DMS) were purchased from Matreya, Inc. (Pleasant Gap, PA, USA). [γ-^{32}P]ATP (3000 Ci/mmol) and [^{14}C]serine (150 mCi/mmol) were from NEN Life Science Products (Boston, MA, USA). Taq polymerase and random hexamer primers were from Takara Bio Co. (Osaka, Japan). Antibodies against ERK, p38 MAPK, ATF2, Tyr^{204}-phosphorylated ERK, Thr^{180}/Tyr^{182}-phosphorylated p38 MAPK, or Thr^{71}-phosphorylated ATF2 were obtained from Cell Signalling Technology Inc. (Boston, MA). Antibodies against PKC α, β, δ, ε, and ζ were from Santa Cruz Biotechnology, Inc. (Santa Cruz, CA, USA). Rabbit antibodies against human SPHK1 (peptide: FIADVDLESEKYRRLGEMRFTLGT) were generated as described previously [32], and antibodies against human SPHK2 were generated in New Zealand White rabbits by injection with recombinant full-length maltose binding protein-fused human SPHK2, which was expressed in *E. coli* and purified as described previously [16]. U0126, PD98059, SB203580, Gö6976 and bisindolylmaleimide (GF 109203X) were from Calbiochem (San Diego, CA, USA). The expression vector containing dominant negative SPHK1 (SPHK1^{G82D}) was a generous gift from Dr. Pitson (University of Adelaide, Australia). The other reagents were of the highest quality available.

2.2. Cell culture and differentiation of HL60 cells

The human leukemia cell lines, HL60 was kindly supplied by Dr. Yukihiro Akao (Gifu International Institute

of Biotechnology). The cells were grown in complete growth medium (RPMI 1640 medium supplemented with 5% fetal bovine serum, 100 units/ml of penicillin, and 100 μg/ml of streptomycin) at 37 °C in a humidified atmosphere containing 5% CO_2. To induce differentiation, 5×10^5 cells/ml were cultured in serum-free RPMI 1640 medium supplemented with 5 μg/ml of insulin and 5 μg/ml of transferrin for 24 h, then treated with 0.5 mM dbcAMP for the indicated time. When the cells were pretreated with drugs before incubation with dbcAMP, the drug was also included in the dbcAMP incubation medium.

2.3. Stable transfection with SPHK1

Human SPHK1 cDNA was cloned by RT-PCR using primers designed using the reported cDNA sequence [33]. pCDNA3.1 vector (Invitrogen) containing cDNA coding for either wild-type SPHK1 or dominant negative SPHK1 (SPHK1DN) (originally names as $SPHK^{G82D}$, [34]) were prepared, and the sequence was confirmed. For stable transfection of HL60 cells, electroporation (300 kV, 400 mF) was applied using 30 μg of expression vector (pcDNA 3.1). After 48 h, the medium was changed to complete growth medium containing 600 μg/ml G418 to expand antibiotic-resistant colonies.

2.4. NBT reduction assay

NBT reduction, an indicator of differentiation, was assayed as described previously [35]. Briefly, 0.8 ml of a solution of 0.125% NBT and 200 nM PMA was added to 2×10^5 cells in 0.2 ml of RPMI 1640 medium and the mixture incubated at 37 °C for 30 min, centrifuged at 1100×*g* for 7 min at room temperature, and resuspended in 200 μl of phosphate-buffered saline (PBS). Aliquots of the samples were stained with Safranin-O for 5 min and the percentage of NBT-positive cells was determined.

2.5. SPHK assay

Cells (5×10^6) were washed twice with cold PBS, centrifuged, and resuspended in 200 μl of 20 mM Tris buffer, pH 7.4, containing 20% (v/v) glycerol, 1 mM mercaptoethanol, 1 mM EDTA, 1 mM sodium orthovanadate, 15 mM sodium fluoride, 10 μg/ml each of leupeptin and aprotinin, 1 mM phenylmethylsulfonyl fluoride (PMSF), and 0.5 mM 4-deoxypyridoxine. The cells were disrupted by freeze–thawing followed by sonication, and the cytosolic fraction prepared by centrifugation at 13,000×g for 30 min at 4 °C. SPHK activity was assayed as described by Olivera et al. [36], with minor modifications. The reaction mixture (200 μl) consisted of 20 mM Tris HCl, pH 7.4, 2.5 mM $MgCl_2$, 0.25 mM EDTA, 5% glycerol, 1.2 mM dithiothreitol, 1 mM Na_3VO_4, and 15 mM NaF, 20 μM sphingosine, and 200 μg of enzyme with or without 0.25% Triton X-100. The reaction (30 min at 37 °C) was started by the addition of 20 μl of [γ-^{32}P] ATP (2 μCi) and 10 mM ATP complex and terminated by the addition of 20 μl of 1 N HCl, followed by 0.8 ml of chloroform/methanol/HCl (100:200:1). After vigorous vortexing, 240 μl of chloroform and 240 μl of 1 M KCl were added and the suspension was centrifuged at 2000×*g* for 10 min at room temperature. The organic phase containing the lipids was removed, concentrated, and applied to a silica gel 60 TLC plate, which was developed in butan-1-ol/acetic acid/water (3:1:1, v/v). The S1P spot was visualized by autoradiography and quantified using a densitometer (Densitograph Atto, Tokyo). Cellular S1P levels were determined as described previously [37].

2.6. RNA extraction and semi-quantitative RT-PCR

Total RNA was isolated from HL60 cells by the acid guanidine thiocyanate method [38]. To quantify SPHK1 gene expression, semi-quantitative RT-PCR was performed as described previously [39]. In preliminary experiments, the amount of cDNA and the number of PCR cycles permitting the linear amplification of SPHK1 and β-actin mRNAs were determined. The human SPHK1 primer sequences were 5′-CACTGAGCGGCGGAACCAC-3′(sense) and 5′-GCTGGACCACAACGGGGGA-3′ (antisense), and the human SPHK2 primer sequences 5′-GAACCGTGCCGAGGCCCAG-3′ (sense) and 5′-CACTGCCCAAGGCCCTGA-3′(antisense). The human β-actin primer sequences were 5′-TCACTCATGAAGATCCTCA-3′ (sense) and 5′-TTCGTGGATGCCACAGGAC-3′ (antisense). The PCR conditions for hSPHK1 and hSPHK2 were 96 °C for 2 min, followed by 30 cycles at 96 °C for 30 s, 32 at 64 °C for 30 s, and 34 at 72 °C for 30 s, while those for β-actin were 96 °C for 2 min, followed by 22 cycles at 96 °C for 15 s, 24 at 58 °C for 30 s, and 26 at 72 °C for 30 s. The intensity of each band was measured using NIH Image (version 6). Within the linear range of PCR amplification, the SPHK1 mRNA levels were evaluated by calculating the SPHK1/β-actin band intensity ratio.

2.7. Western blot analysis

Cells were cultured for 24 h in serum-free RPMI 1640 medium supplemented with 5 μg/ml each of insulin and transferrin, treated with 0.5 mM dbcAMP for the indicated time, then harvested by centrifugation at 3000×*g* for 5 min at 4 °C. To prepare whole cell lysates, the cells were resuspended in ice-cold lysis buffer (1% Nonidet P-40, 0.5% sodium desoxycholate, 1% sodium dodecyl sulfate, 1 mM EDTA, 1 mM EGTA, 150 mM NaCl, 50 mM Tris, 3 mM MgCl2, 1 mM PMSF, 20 μg/ml of leupeptin, 20 mM β-glycerophosphate, 1 mM sodium fluoride, and 1 mM sodium orthovanadate, pH 7.4), and sonicated. To prepare the membrane fractions, the cells were resuspended in 50 mM Tris–HCl buffer, pH 7.4, containing 1 mM PMSF, and 20 μg/ml of leupeptin, sonicated, then centrifuged at 100,000×*g* for 60 min at 4 °C, and the pellet resuspended

in the lysis buffer. Protein concentrations were assayed using the Bradford protein assay reagent (Bio Rad) with bovine serum albumin (BSA) as the standard. Total cell lysates and membrane preparations (50–100 μg of protein) were subjected to electrophoresis on 10% SDS-polyacrylamide gels and transferred to polyvinylidene difluoride membranes (Millipore), which were then blocked with 5% BSA. The phosphorylation of ERK and p38 MAPK and the total amounts of ERK, p38 MAPK, SPHK1, SPHK2, or PKC α, β, δ, ε, or ζ were determined by immunoblotting with rabbit polyclonal antibodies against phosphorylated ERK, phosphorylated p38 MAPK, ERK, p38 MAPK, SPHK1, SPHK2, or PKC α, β, δ, ε, and ζ, respectively, followed by horseradish peroxidase-linked secondary antibody. After repeated washes, bound antibodies were detected using the ECL Western blotting detection system (ParkinElmer Life Sci. Inc., Boston, MA).

3. Results

3.1. Changes in SPHK activity and SPHK1 and SPHK2 mRNA and protein levels during dbcAMP-induced granulocytic differentiation of HL60 cells

To determine whether SPHK was involved in cell differentiation, we examined changes in SPHK activity and mRNA levels of SPHK1 and SPHK2 in HL60 cells at various stages during differentiation initiated by the addition of 0.5 mM dbcAMP. We measured SPHK activity in both the absence and presence of 0.25% Triton X-100, conditions which, respectively, measure the combined activity of SPHK1 and SPHK2 or the activity of SPHK1 alone [16], and found no significant difference between the two values during the dbcAMP-induced differentiation of HL60 cells (data not shown), suggesting that only SPHK1 was present in these cells. As shown in Fig. 1A, SPHK activity showed a time-dependent increase, reaching levels approximately 400% of those in undifferentiated cells after 24 h of treatment, then increasing more slowly up to 72 h of treatment (430% and 450% of control levels of at 48 and 72 h, respectively). This increase in SPHK activity was accompanied by an increase in intracellular S1P levels to 200% and 250% of control levels at 24 h and 72 h, respectively (Fig. 1B). SPHK1 mRNA levels, measured by semi-quantitative PCR analysis, also showed a time-dependent increase after dbcAMP treatment, reaching 400% of control levels at 24 h (Fig. 2A,C). SPHK2 mRNA was undetectable in HL60 cells by RT-PCR using the hSPHK2 primers (Fig. 2B). Western blot analysis showed an increase in SPHK1 protein to 350% of control levels after 48 h of dbcAMP treatment (Fig. 2D). No SPHK2 protein was detectable in either undifferentiated or differentiated HL60 cells. These findings, together with the results of the SPHK assay in the absence and presence of Triton X-100, show that the increase in SPHK activity was due to increased levels of SPHK1 protein.

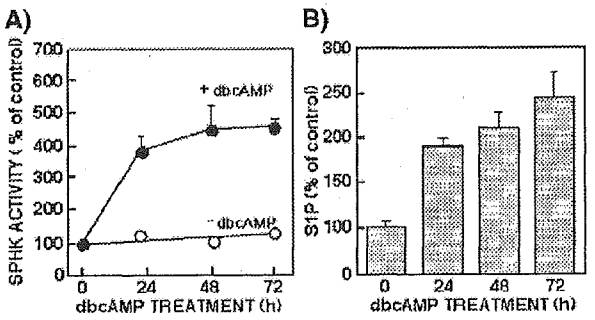

Fig. 1. Changes in SPHK activity and intracellular S1P levels during dbcAMP-induced HL60 cell differentiation. HL60 cells were incubated with 0.5 mM dbcAMP for the indicated time, then SPHK activity (A) and cellular levels of S1P (B) were measured as described in the Materials and methods. The control SPHK activity was 3.1±1.2 pmol/min/mg protein and the S1P level was 11.5±2.5/10^6 cells. The results are expressed as the mean±S.D. for three experiments, each performed in duplicate.

To further assess the involvement of SPHK in HL60 cell differentiation, we examined the effects of the potent SPHK inhibitor, DMS. Treatment of control HL60 cells with DMS for 72 h inhibited the subsequent dbcAMP-induced increase in SPHK activity in a concentration-dependent manner, with 90% inhibition at 5 μM (Fig. 3A), at which concentration the cells were more than 95% viable, as assessed by Trypan blue exclusion (data not shown), in agreement with a previous report [40]. When HL60 cells were treated with 0.5 mM dbcAMP, the percentage of NBT-reducing cells (a measure of differentiation) increased in a time-dependent manner (Fig. 3B) and this effect was suppressed by 90% by pretreatment of the cells for 1 h with 5 μM DMS, providing additional evidence for the involvement of SPHK1 in the dbcAMP-induced granulocytic differentiation of HL60 cells.

3.2. Activation of MAPK during dbcAMP-induced granulocytic differentiation of HL60 cells

The activation of ERK1/2 and p38 MAPK during dbcAMP-induced differentiation was examined using antibodies specific for phosphorylated forms of ERK or p38 MAPK. As shown in Fig. 4A, time-course analysis showed that dbcAMP treatment resulted in a marked increase in the phosphorylation of both ERK and p38 MAPK after 24 h of treatment. After 72 h of dbcAMP treatment, the phosphorylation of ERK1/2 and p38 MAPK was increased to 500% and 200% of control levels, respectively, whereas the total amounts of ERK1/2 and p38 MAPK protein were not significantly affected by the same treatment.

To determine whether the dbcAMP-induced activation of ERK1/2 was due to MEK activity, the cells were preincubated for 1 h with 10 μM U0126, a potent MEK inhibitor, before incubation for 72 h with 0.5 mM dbcAMP. As shown in Fig. 4B, U0126 pretreatment completely blocked dbcAMP-induced ERK1/2 phosphorylation, but had no effect on total

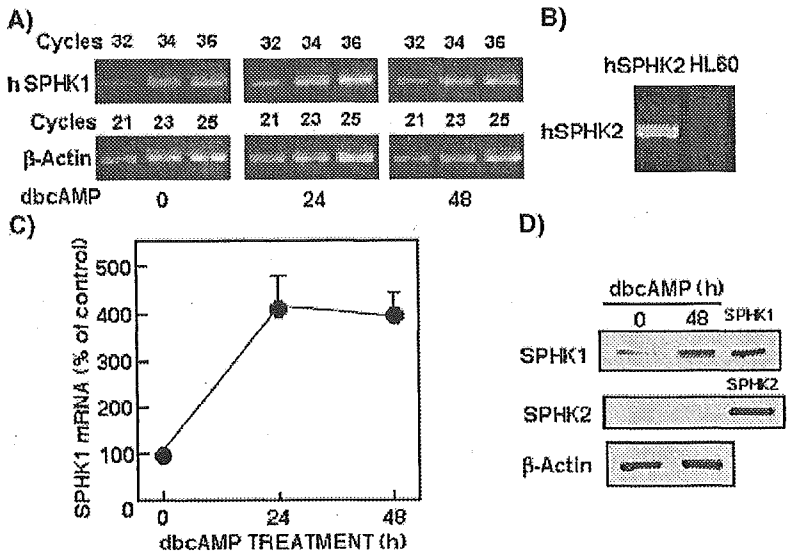

Fig. 2. Increase in SPHK1 mRNA and protein levels during dbcAMP-induced HL60 cell differentiation. (A) SPHK1 mRNA levels in HL60 cells incubated with 0.5 mM dbcAMP for the indicated times and (B) SPHK2 mRNA levels in SPHK2-transfected HEK 293 cells and in HL60 cells incubated with 0.5 mM dbcAMP for 48 h were determinated as described in the Materials and methods. (C) SPHK1 mRNA levels in HL60 cells incubated with 0.5 mM dbcAMP for 24 and 48 h expressed as a percentage of the control levels. (D) HL60 cells incubated for 48 h with 0.5 mM dbcAMP and HEK 293 cells overexpressing SPHK1 or SPHK2 were lysed, and the lysates were subjected to Western blot analysis using antibodies against SPHK1 or SPHK2, respectively, as described in the Materials and methods. β-Actin was used as loading control. The results are the representative of those from three independent experiments.

ERK protein levels, showing that ERK1/2 activation was mediated by MEK. Pretreatment with the p38 MAPK inhibitor, SB203580, had an inhibitory effect on the downstream ATF2 activation induced by dbcAMP treatment, but did not affect dbcAMP-induced ERK1/2 activation.

To examine the involvement of MAPKs in dbcAMP-induced differentiation, HL60 cells were preincubated for 1 h with 10 μM U0126 or 10 μM SB203580 prior to dbcAMP addition. Preincubation with U0126 resulted in complete suppression of dbcAMP-induced differentiation, assessed as the percentage of NBT-reducing cells, whereas SB203580 had no significant effect (Fig. 4C). These results suggest that the MEK/ERK pathway, but not the p38 MAPK pathway, is important for the granulocytic differentiation of HL60 cells.

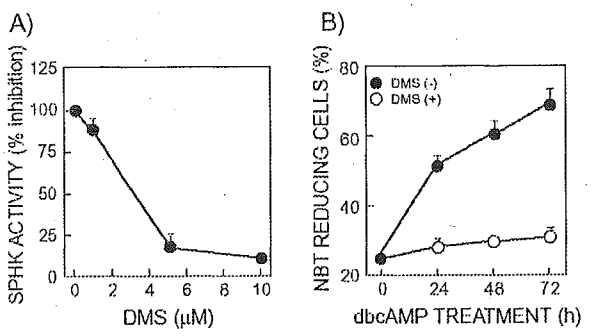

Fig. 3. DMS pretreatment inhibits the dbcAMP-induced increase in SPHK activity and differentiation. (A) HL60 cells were incubated for 1 h with the indicated concentration of DMS, then for 72 h with 0.5 mM dbcAMP in the continued presence of DMS. SPHK activity was measured as described in the Materials and methods and expressed as a percentage of the value in the absence of DMS. (B) After incubation of the cells for 1 h with or without 5 μM DMS, then incubation for the indicated time with 0.5 mM dbcAMP with or without DMS, the percentage of NBT-reducing cells was measured to monitor cell differentiation. The results are expressed as the mean±S.D. for three experiments, each performed in duplicate.

3.3. ERK activation occurs downstream of SPHK activation during dbcAMP-induced differentiation

To determine the relationship between SPHK and MAPKs in the dbcAMP-induced differentiation of HL60 cells, the effects of DMS on the dbcAMP-induced activation of these enzymes were examined. DMS inhibited the ERK1/2 activation seen after 72 h of treatment with 0.5 mM dbcAMP in a concentration-dependent manner (Fig. 5A), with approximately 80% inhibition using 5 μM DMS, but had little effect on dbcAMP-induced p38 MAPK activation (Fig. 5B). These results strongly suggest that ERK1/2 activation, but not p38 MAPK activation, occurs downstream of SPHK activation.

DMS has been reported to affect PKC activity [41] and it has been suggested that SPHK activity is regulated by the activation of phospholipase D (PLD), which is mediated by PKC in HL60 cells [11,42]. We have previously shown that PKCα and βI are translocated to the membrane during the dbcAMP-induced differentiation of HL60 cells and that membrane-associated PKCα and βI are involved in PLD activation [23,24]. We therefore examined the effect of DMS on the translocation of PKC isozymes to the membrane. As shown in Fig. 6, dbcAMP treatment for 72 h induced an increase in membrane levels of PKCα and PKCβI, but not those of PKCβII, PKCδ, PKCε or PKCζ,

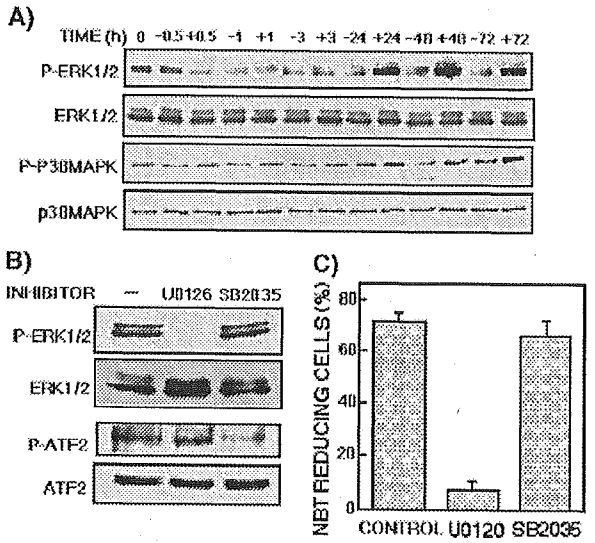

Fig. 4. Effects of MEK and p38 MAPK inhibitors on the MAPK activation during the dbcAMP-induced differentiation of HL60 cells. (A) HL60 cells were incubated with (+) or without (−) 0.5 mM dbcAMP for the indicated time, then the cell lysates were subjected to Western blot analysis using antibodies reactive with either phosphorylated or total ERK or P38 MAPK, respectively, as described in the Materials and methods. (B) HL60 cells were incubated for 1 h with or without 10 μM U0126 or 10 μM SB203580, then for 72 h with 0.5 mM dbcAMP in the presence or absence of the same drug, then cell lysates were subjected to Western blotting using antibodies reactive with either phosphorylated or total ERK or ATF2. The results in A and B are representative of those from three independent experiments. (C) After incubation for 1 h with or without 10 μM U0126 or 10 μM SB203580, followed by incubation for 72 h with 0.5 mM dbcAMP in the presence or absence of the same drug, the percentage of NBT-reducing cells was measured. The results are expressed as the mean±S.D. for three different experiments, each performed in duplicate.

and this increase was not inhibited by DMS pretreatment. Furthermore, pretreatment with a PKC inhibitor (Gö6976 or GF 109203X) did not inhibit the dbcAMP-mediated induction of ERK activation, but rather increased the effect (Fig. 7A). In addition, these PKC inhibitors did not affect the dbcAMP-induced increase in SPHK activity and the granulocytic differentiation of HL60 cells (data not shown). These results suggest that PKC is not involved in the dbcAMP-induced increase in SPHK and ERK activation in HL60 cells.

Our previous study has demonstrated that PMA-induced SPHK1 gene expression in a human leukemia cell line, MEG-01, is ERK-dependent [39]. We therefore examined the effect of MAP kinase inhibitors on the dbcAMP-induced increase in SPHK activity. The increase in SPHK activity during the dbcAMP-induced differentiation of HL60 cells was not affected by the preincubation of the cells with MEK inhibitors, U0126 and PD90859, or p38MAP kinase inhibitor SB203580 (Fig. 7B), showing that it was not mediated via the MAP kinase activation pathway.

To confirm that SPHK was involved in granulocytic differentiation and ERK activation, wild-type SPHK1 (W) and the dominant negative (DN) SPHK1 were stably overexpressed in HL60 cells and clones overexpressing wild-type SPHK1 (W 6 and W8) or DN SPHK1 (DN6 and DN9) were selected. Western blots showed that SPHK1 expression was increased in all overexpressing clones (W6, W8, DN6, and DN9) (Fig. 8A). In addition, SPHK activity (shown by S1P production) was markedly higher (approximately 300% of control levels) in the SPHK1-overexpressing cells than in the control cells, but was lower than in

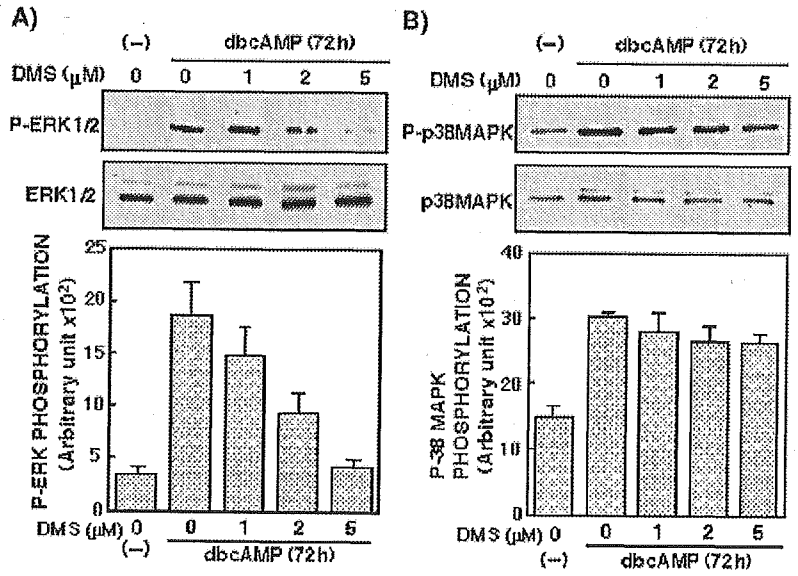

Fig. 5. Effect of DMS on MAPK phosphorylation in differentiated HL60 cells. HL60 cells were incubated for 1 h with the indicated concentration of DMS, then for 72 h with or without (−) 0.5 mM dbcAMP in the continued presence of DMS. Phosphorylation and total expression of ERKs (A) and p38 MAPK (B) were measured by Western blot analysis using specific antibodies as described in the Materials and methods. Upper panel, representative blot for three independent experiments; lower panel, densitometric data expressed as the mean±S.D. for three experiments.

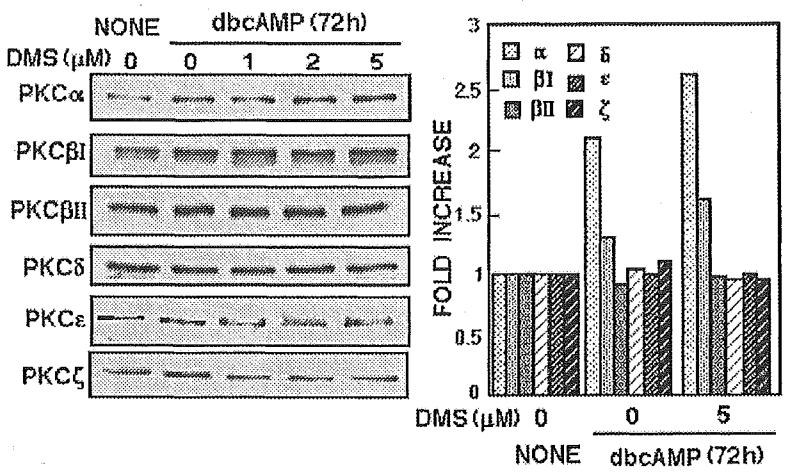

Fig. 6. Effect of DMS on the membrane translocation of PKC isozymes in differentiating HL60 cells. The cells were incubated for 1 h with the indicated concentration of DMS, then for 72 h with 0.5 mM dbcAMP in the continued presence of DMS and the membrane fractions were isolated and subjected to Western blot analysis using specific PKC isozyme antibodies as described in the Materials and methods. The left panel shows results representative of those for two independent experiments and the right panel shows the mean densitometric data for the two experiments expressed as a fold increase compared to the control.

control cells in the SPHK DN-expressing cells. Western blots (Fig. 8A) also showed that levels of phosphorylated ERK1/2, but not of total ERK proteins, were considerably increased in the wild-type SPHK1-overexpressing cells, in contrast, levels of phosphorylated ERK1/2 in the SPHK1DN-overexpressing HL60 cells were lower than those in control cells. As shown in Fig. 8B, differentiation after treatment for 72 h with dbcAMP was significantly increased in the SPHK1-overexpressing cells suppressed in SPHKDN-overexpressing cells compared to control cells. These findings provide additional evidence that SPHK1 plays an important role in dbcAMP-induced ERK activation and granulocytic differentiation in HL60 cells.

Several lines of evidence indicate that S1P produced by SPHK activation acts both intracellularly and extracellularly, and that extracellular S1P, acting through a G protein-coupled receptor, induces MAPK activation, which is inhibited by pertussis toxin (PTX) [1,2]. To determine whether the S1P produced by SPHK activation during dbcAMP-induced MAPK activation acted as a second messenger or via a G protein-coupled receptor, the effect of PTX was tested. As shown in Fig. 8C, PTX pretreatment

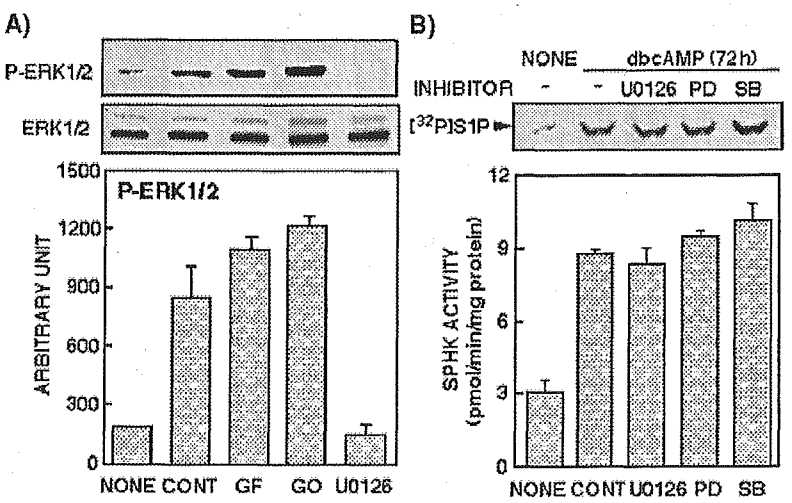

Fig. 7. Effect of PKC inhibitors on ERK phosphorylation and a MAP kinase inhibitor on SPHK activity in dbcAMP-treated HL60 cells. (A) The cells were incubated for 1 h with or without PKC inhibitor [1 μM of Gö6976 (GO), 5 μM GF 109203X (GF)], or a MEK inhibitor U0126 (10 μM), then for 72 h with 0.5 mM dbcAMP with or without the same inhibitor. Phosphorylation and total expression of ERKs were measured by Western blot analysis using specific antibodies as described in the Materials and methods. (B) HL60 cells incubated for 1 h with or without 10 μM U0126, 50 μM of PD90859, or 10 μM SB203580, then for 72 h with or without (–) 0.5 mM dbcAMP, and with or without the same inhibitor, and SPHK activity measured as described in the Materials and methods. Upper panel, representative blot for three independent experiments; lower panels, densitometric data expressed as the mean±S.D. for the three experiments.

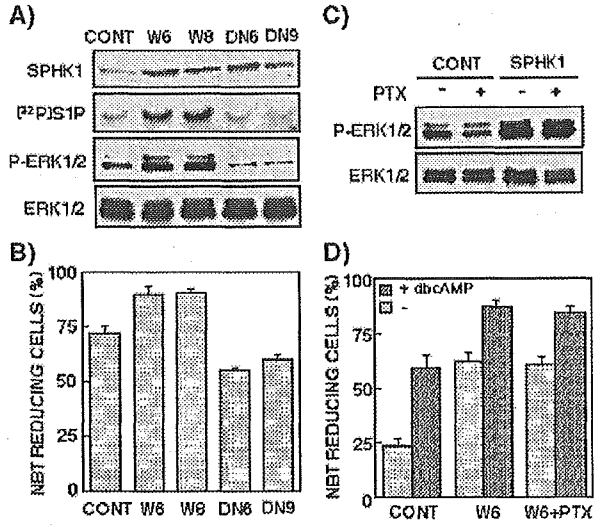

Fig. 8. Effect of wild type and dominant negative SPHK1 overexpression on dbcAMP-induced differentiation and ERK activation in HL60 cells. The cells were transfected with wild-type (W) or dominant negative (DN) SPHK1 pcDNA 3.1 and transformants selected using G418. Two clones overexpressing the wild-type (W6 and W8) or dominant negative (DN6 and DN9) were selected, and tested. (A) Basal levels of SPHK1 protein, SPHK activity, and ERK phosphorylation in control (CONT, no transfection) or SPHK1-overexpressing cells (W6, W8, DN6 and DN9) were measured as described in the Materials and methods. The results are representative of those for three independent experiments. (B) Percentage of NBT-reducing cells after treatment with 0.5 mM dbcAMP for 72 h. The results are expressed as the mean±S.D. for three different experiments. (C) Control and W6 cells were incubated for 1 h with or without 100 ng/ml of PTX, then for 48 h with 0.5 mM dbcAMP in the continued presence of PTX, and the phosphorylation of ERK1/2 was measured as described in the Materials and methods. The results are representative of three independent experiments. (D) Control and W6 cells were incubated for 1 h with or without 100 ng/ml of PTX, then for 48 h with or without 0.5 mM dbcAMP in the continued presence of PTX, and the percentage of NBT reducing cells measured as described in the Materials and methods. The results are expressed as the mean±S.D. for three different experiments.

had no inhibitory effect on the dbcAMP-induced phosphorylation of ERK1/2 in either the control or SPHK1-overexpressing cells (W6). As shown in Fig. 8D, the percentage of NBT-reducing cells in SPHK1-overexpressing W6 cells was much higher than that in control cells even in the absence of dbcAMP, and the differentiation of the control and W6 cells was not affected by PTX treatment in either the presence or absence of dbcAMP. These results suggested that the increase in ERK activation and granulocytic differentiation due to SPHK1 overexpression is not induced via a G-protein coupled receptor in HL60 cells.

4. Discussion

In mammals, two types of SPHK have been identified, SPHK1 and SPHK2 [15,16]. Cell proliferation and survival are enhanced by SPHK1 overexpression, whereas SPHK2 overexpression induces cell death [2]. In the present study, we demonstrated that SPHK activity was greatly increased during the dbcAMP-induced granulocytic differentiation of HL60 cells and that this was due to the increased mRNA and protein levels of SPHK1, but not SPHK2, which was not expressed in HL60 cells. This result is in agreement with the results of our previous study in which human leukemia HEL cells were more strongly stained by anti-SPHK1 antibody than were undifferentiated cells and showed increased SPHK activity after PMA-induced differentiation [19]. Furthermore, we have recently found that prolonged (24 h) treatment of megakaryocytic cells with PMA upregulates SPHK1 gene expression through PMA-responsive elements in the 5′ promoter region of the gene [39]. This finding led us to speculate that treatment of HL60 cells with dbcAMP induced the upregulation of SPHK1 gene expression. However, the mechanism of SPHK1 activation induced by dbcAMP is not clear, since previous studies have shown that SPHK1 is activated by PKC or MAP kinase [30,41,42], whereas, in this study, the increase in dbcAMP-induced SPHK1 was found to be independent of PKC and MAP kinase.

There is ample evidence that the activation of the MAPK signaling pathway is associated with cell differentiation [25–29]. In the all-*trans* retinoic acid-induced granulocytic differentiation and the 1,25-dihydroxyviatmin D3-induced monocytic differentiation of HL60 cells, MEK-dependent ERK activation is needed for cell differentiation and growth arrest [25,26]. In the present study, we demonstrated that, in HL60 cells, dbcAMP caused sustained ERK activation during differentiation and that the inhibition of the activation of MEK/ERKs abolished dbcAMP-induced differentiation. These results show that sustained ERK activation is required for the granulocytic differentiation of HL60 cells. However, the role of p38 MAPK in cell differentiation seems to be more complex. p38 MAPK suppresses the monocytic differentiation of NB-4 and HL60 leukemia cells [27,28], but promotes the erythroid differentiation of K562 cells [29]. In the present study, treatment of HL60 cells with dbcAMP induced a significant p38 MAPK activation, although this was less marked than the ERK activation. However, p38 MAPK is not involved in the dbcAMP-induced granulocytic differentiation of HL60 cells, since p38 MAPK inhibition by SB203580 had no effect on differentiation.

Interestingly, in HL60 cells, the dbcAMP-induced activation of ERKs, but not that of p38 MAPK, was markedly suppressed by the SPHK inhibitor, DMS, indicating that MEK/ERK activation was upregulated by SPHK1. A similar relationship between SPHK and ERK was observed in our previous study, which demonstrated that SPHK inhibition by DMS resulted in the downregulation of ERKs activation in, and the differentiation of, hepatoma Huh-7 cells [17]. It has been reported that PKC is implicated in SPHK and ERK activation, and that DMS inhibits PKC activity [30,41,42]. However, in this study, we have demonstrated that PKC was not involved in dbcAMP-induced ERK activation and granulocytic differentiation,

since PKC inhibitors had no significant effect on ERK activation. Collectively, these findings suggest that SPHK plays an important role in cell differentiation by regulating the downstream MEK/ERK pathway. However, the precise mechanism involved in the upregulation of the MEK/ERK pathway via SPHK activation remains to be elucidated.

The overexpression of SPHK1 in NIH3T3 cells or HEK293 cells markedly increases intracellular S1P levels and enhances proliferation by promoting the G1 to S phase transition [13] and suppresses serum deprivation- or ceramide-induced apoptosis [3], while treatment of HL60 cells with 1,25 dihydroxyvitamin D3 suppresses ceramide-induced apoptosis by increasing SPHK activity, leading to increased levels of S1P [22]. Furthermore, a recent study [30] has shown that, in the T24 human bladder carcinoma cell line, the dominant negative SPHK1 or small interfering RNA targeted at SPHK1 blocks the VEGF-induced Ras-GTP accumulation and ERK activation and that VEGF induces DNA synthesis via the pathway which sequentially involves PKC, SPHK1, Ras, Raf, and ERKs. The same study also shows that the signaling pathway used by VEGF is different from that used by the S1P receptor, since no S1P secretion was detected, and that the intracellular S1P generated by SPHK1 activation by VEGF stimulation leads to the activation of downstream signaling that does not involve S1P receptors. It has also been reported that the survival-promoting effects of SPHK occur in the absence of detectable S1P secretion and are PTX-independent [4,10,30]. In the present study, we demonstrated that the SPHK inhibitor, DMS, caused a concomitant block of the differentiation and ERK activation induced by dbcAMP in HL60 cells. Furthermore, we showed that the overexpression of wild-type SPHK1, but not dominant negative form, stimulated ERK activation and granulocytic differentiation even in the absence of dbcAMP and that the differentiation due to SPHK1 overexpression was PTX-independent. These results suggest that, in the dbcAMP-induced granulocytic differentiation of HL60 cells, SPHK1 plays an important role by upregulating ERK activation via a PTX-independent pathway. This finding is consistent with the reduced expression of the S1P receptor in differentiated HL60 cells [43,44].

In summary, the present study demonstrates that treatment of HL60 cells with dbcAMP to induce granulocytic differentiation results in a sustained increase in SPHK activity, which is due to increased SPHK1 protein levels and the activation of ERKs, but not of p38 MAPK. It also shows that the ERK activation required for differentiation is controlled by SPHK activity and is not inhibited by PTX.

Acknowledgements

This work was supported in part by Grants-in-Aid for Scientific Research (B) (09480162) and (C) (14580646) from the Ministry of Education, Science, Sports, and Culture of Japan.

Appendix A. Supplementary figure

Supplementary data associated with this article can be found, in the online version, at doi:10.1016/j.bbalip.2004.12.006.

References

[1] S. Pyne, N.J. Pyne, Sphingosine 1-phosphate signaling in mammalian cells, Biochem. J. 349 (2000) 385–402.
[2] S. Spiegel, S. Milstein, Sphingosine-1-phosphate: an enigmatic signalling lipid, Nat. Rev., Mol. Cell Biol. 4 (2003) 397–407.
[3] O. Cuvillier, G. Pirianov, B. Kleuser, P.G. Vanek, O.A. Coso, J.S. Gutkind, S. Spiegel, Suppression of ceramide-mediated programmed cell death by sphingosine-1-phosphate, Nature 381 (1996) 800–803.
[4] L.C. Edsall, G.G. Pirianov, S. Spiegel, Involvement of sphingosine-1-phosphate in nerve growth factor-mediated neuronal survival and differentiation, J. Neurosci. 17 (1997) 6952–6960.
[5] A. Kihara, M. Ikeda, Y.K. Ariya, E.-Y. Lee, Y.-M. Lee, Y. Igarashi, Sphingosine-1-phosphate lyase is involved in the differentiation of F9 embryonal carcinoma cells to primitive endoderm, J. Biol. Chem. 278 (2003) 14578–14585.
[6] A. Berger, R. Bittman, R.R. Schmidt, S. Spiegel, Structural requirements of sphingosylphosphocholine and sphingosine-1-phosphate for stimulation of activator protein-1 activity, Mol. Pharmacol. 50 (1996) 451–457.
[7] A.C. Mackinnon, A. Buckley, E.R. Chilvers, A.G. Rossi, C. Haslett, T. Swthi, Sphingosine kinase: a point of convergence in the action of diverse neutrophil priming agents, J. Immunol. 169 (2002) 6394–6400.
[8] Y. Banno, H. Fujita, Y. Ono, S. Nakashima, Y. Ito, N. Kuzumaki, Y. Nozawa, Differential phospholipase D activation by bradykinin and sphingosine 1-phosphate in NIH 3T3 fibroblasts overexpressing gelsolin, J. Biol. Chem. 274 (1999) 27385–27391.
[9] M.J. Kluk, T. Hla, Signaling of sphingosine-1-phosphate via the S1P/EDG-family of G-protein-coupled receptors, Biochim. Biophys. Acta 1582 (2002) 72–80.
[10] A. Olivera, S. Spiegel, Sphingosine-1-phosphate as second messenger in cell proliferation induced by PDGF and FCS mitogens, Nature 365 (1993) 557–560.
[11] A. Melendez, R.A. Floto, D.J. Gillooly, M.M. Harnett, J.M. Allen, FcγRI coupling to phospholipase D initiates sphingosine kinase-mediated calcium mobilization and vesicular trafficking, J. Biol. Chem. 273 (1998) 9393–9402.
[12] P. Xia, L. Wang, J.R. Gamble, M.A. Vadas, Activation of sphingosine kinase by tumor necrosis factor-α inhibits apoptosis in human endothelial cells, J. Biol. Chem. 274 (1999) 3499–34505.
[13] P. Xia, R.G. Gamble, L. Wang, S.M. Pitson, P.A.B. Moretti, B.W. Wattenberg, R.J. D'Andrea, M.A. Vadas, An oncogenic role of sphingosine kinase, Curr. Biol. 10 (2000) 1527–1530.
[14] D.M.Zu Heringdorf, H. Lass, R. Alemany, K.T. Laser, E. Neumann, C. Zhang, M. Schmidt, U. Rauen, K.H. Jakobs, C.J. van Koppen, Sphingosine kinase-mediated Ca^{2+} signalling by G-protein-coupled receptors, EMBO J. 17 (1998) 2830–2837.
[15] T. Kohama, A. Olivera, L. Edsall, M.M. Nagiec, R. Dickson, S. Spiegel, Molecular cloning and functional characterization of murine sphingosine kinase, J. Biol. Chem. 273 (1998) 23722–23728.
[16] H. Liu, M. Sugiura, V.E. Nava, L.C. Edsall, K. Kono, S. Poulton, S. Milstein, T. Kohama, S. Spiegel, Molecular cloning and functional characterization of a novel mammalian sphingosine kinase type 2 isoform, J. Biol. Chem. 275 (2000) 19513–19520.
[17] Y. Osawa, M. Nagaki, Y. Banno, Y. Nozawa, H. Motiwaki, S. Nakashima, Sphingosine kinase regulates hepatoma cell differentiation: roles of hepatocyte nuclear factor and retinoid receptor, Biochem. Biophys. Res. Commun. 286 (2001) 673–677.

[18] Y. Banno, M. Kato, A. Hara, Y. Nozawa, Evidence for the presence of multiple forms of Sph kinase in human platelets, Biochem. J. 335 (1998) 301–304.
[19] T. Murate, Y. Banno, K. T-Koizumi, K. Watanabe, N. Mori, A. Wada, Y. Igarashi, A. Takagi, T. Kojima, H. Asano, Y. Akao, S. Yoshida, H. Saito, Y. Nozawa, Cell type-specific localization of sphingosine kinase 1a in human tissues, J. Histochem. Cytochem. 49 (2001) 845–855.
[20] Y. Fukuda, A. Kihara, Y. Igarashi, Distribution of sphingosine kinase activity in mouse tissues: contribution of SPHK1, Biochem. Biophys. Res. Commun. 309 (2003) 155–160.
[21] S.J. Collins, The HL60 promyelocytic leukemia cell line proliferation, differentiation, and cellular oncogene expression, Blood 70 (1987) 1233–1244.
[22] B. Kleuser, O. Cuvillier, S. Spiegel, 1 Alpha, 25-dihydroxyvitamin D3 inhibits programmed cell death in HL60 cells by activation of sphingosine kinase, Cancer Res. 58 (1998) 1817–1824.
[23] K. Ohguchi, Y. Banno, S. Nakashima, Y. Nosawa, Regulation of membrane-bound phospholipase D by protein kinase C in HL60 cells, J. Biol. Chem. 271 (1996) 4366–4372.
[24] K. Ohguchi, S. Nakashima, Z. Tan, Y. Banno, S. Dohi, Y. Nozawa, Increased activity of small GTP-binding protein-dependent phospholipase D during differentiation in human promyelocytic leukemic HL60 cells, J. Biol. Chem. 272 (1997) 1990–1996.
[25] M.B. Miranda, T.F. McGuire, D.E. Johnson, Importance of MEK-1/-2 signaling in monocytic and granulocytic differentiation of myeloid cell lines, Leukemia 16 (2002) 683–692.
[26] A. Yen, M.S. Roberson, S. Varvayanis, A.T. Lee, Retinoic acid induced mitogen-activated protein (MAP)/extracellular signal-regulated kinase (ERK) kinase-dependent MAP kinase activation needed to elicit HL-60 cell differentiation and growth arrest, Cancer Res. 58 (1998) 3163–3172.
[27] Y. Alsayed, S. Uddin, N. Mahmud, F. Lekmine, D.V. Kalvakolanu, S. Minucci, G. Bokoch, L.C. Platanias, Activation of Rac1 and the p38 mitogen-activated protein kinase pathway in response to all-*trans*-retinoic acid, J. Biol. Chem. 276 (2001) 4012–4019.
[28] X. Wang, J. Rao, G.P. Studzinski, Inhibition of p38 MAP kinase activity up-regulates multiple MAP kinase pathways and potentiates 1,25-dihydroxyvitamin D3-induced differentiation of human leukemia HL60 cells, Exp. Cell Res. 258 (2000) 425–437.
[29] J.M. Ayala, S. Goyal, N.J. Liverton, D.A. Claremon, S.J. O'Keefe, W.A. Hanlon, Serum-induced monocyte differentiation and monocyte chemotaxis are regulated by the p38 MAP kinase signal transduction pathway, J. Leukoc. Biol. 67 (2000) 869–875.
[30] X. Shu, W. Wu, R.D. Mosteller, D. Brock, Sphingosine kinase mediates vascular endothelial growth factor-induced activation of ras and mitogen-activated protein kinases, Mol. Cell. Biol. 22 (2002) 7758–7768.
[31] C.S. Rani, F. Wang, E. Fuior, A. Berger, J. Wu, T.W. Sturgill, D. Beitner-Johnson, D. LeRoith, L. Varticovski, S. Spiegel, Divergence in signal transduction pathways of platelet-derived growth factor (PDGF) and epidermal growth factor (EGF) receptors. Involvement of sphingosine 1-phosphate in PDGF but not EGF signaling, J. Biol. Chem. 272 (1997) 10777–10783.
[32] A.J. Melendez, A.K. Khaw, Dichotomy of Ca^{2+} signals triggered by different phospholipids pathways in antigen stimulation of human mast cells, J. Biol. Chem. 277 (2002) 17255–17262.
[33] V.E. Nava, E. Lacana, S. Poulton, H. Liu, M. Sugiura, K. Kono, S. Milstien, T. Kohama, S. Spiegel, Functional characterization of human sphingosine kinase-1, FEBS Lett. 473 (2000) 81–84.
[34] S.M. Pitson, P.B. Moretti, J.R. Zebol, P. Xia, J.R. Gamble, M.A. Vadas, R.J. D'Andrea, B.W. Watternberg, Expression of a catalytically inactive sphingosine kinase mutant blocks agonist-induced sphingosine kinase activation. A dominant-negative sphingosine kinase, J. Biol. Chem. 275 (2000) 33945–33950.
[35] T.J. Chaplinski, J.E. Niedel, Cyclic nucleotide-induced maturation of human promyelocytic leukemia cells, J. Clin. Invest. 70 (1982) 953–964.
[36] A. Olivera, J. Rosenthal, S. Spiegel, Effect of acidic phospholipids on sphingosine kinase, J. Cell. Biochem. 60 (1996) 529–537.
[37] Y. Osawa, Y. Banno, M. Nagaki, D.A. Brenner, T. Naiki, Y. Nozawa, S. Nakashima, H. Moriwaki, TNF-α-induced sphingosine 1-phosphate inhibits apoptosis through a phosphatidylinositol 3-kinase/Akt pathway in human hepatocytes, J. Immunol. 167 (2001) 173–180.
[38] J.M. Chirgwin, A.E. Przybyla, R.J. MacDonald, W.J. Rutter, Isolation of biologically active ribonucleic acid from sources enriched in ribonuclease, Biochemistry 18 (1979) 5294–5299.
[39] Y. Nakade, Y. Banno, K. T-koizumi, K. Hagiwara, S. Sobue, M. Koda, M. Suzuki, T. Kojima, A. Takagi, H. Asano, Y. Nozawa, T. Murate, Regulation of sphingosine kinase 1 gene expression by protein kinase C in a human leukemia cell line, MEG-01, Biochim. Biophys. Acta 1635 (2003) 104–116.
[40] D.B. Jendiroba, J. Klostergaard, A. Keyhani, L. Pagliaro, E.J. Freireich, Effective cytotoxicity against human leukemias and chemotherapy-resistant leukemia cell lines by *N*, *N*-dimethylsphingosine, Leuk. Res. 26 (2002) 301–310.
[41] L.C. Edsall, J.R. Van Brocklyn, O. Cuvillier, B. Kleuser, S. Spiegel, *N,N*-dimethylsphingosine is a potent competitive inhibitor of sphingosine kinase but not of protein kinase C: modulation of cellular levels of sphingosine 1-phosphate and ceramide, Biochemistry 37 (1998) 12892–12898.
[42] K.B. Johnson, K.P. Becker, M.M. Facchinetti, Y.A. Hannun, L.M. Obeid, PKC-dependent activation of sphingosine kinase 1 and translocation of the plasma membrane. Extracellular release of sphingosine 1-phosphate induced by phorbol 12-myristate (PMA), J. Biol. Chem. 277 (2002) 35257–35262.
[43] K. Sato, N. Murata, J. Koh, H. Tomura, H. Nochi, K. Tamoto, M. Osada, H. Ohta, Y. Tokumitsu, M. Ui, F. Okajima, Downregulation of mRNA expression of Edg-3, a putative sphingosine 1-phosphate receptor coupled to Ca^{2+} signaling, during differentiation of HL-60 leukemia cells, Biochem. Biophys. Res. Commun. 253 (1998) 253–256.
[44] J.R. Van Brocklyn, M.J. Lee, R. Menzeleev, A. Olivera, L. Edsall, O. Cuvillier, D.M. Thomas, P.J. Coopman, S. Thangada, C.H. Liu, T. Hla, S. Spiegel, Dual actions of sphingosine-1-phosphate: extracellular through the Gi-coupled receptor Edg-1 and intracellular to regulate proliferation and survival, J. Cell Biol. 142 (1998) 229–240.

Available online at www.sciencedirect.com
SCIENCE DIRECT
Biochimica et Biophysica Acta 1727 (2005) 125–133
BIOCHIMICA ET BIOPHYSICA ACTA
BBA
http://www.elsevier.com/locate/bba

Transcriptional regulation of FKLF-2 (KLF13) gene in erythroid cells

Ayako Mitsuma[a], Haruhiko Asano[a,*], Tomohiro Kinoshita[a], Takashi Murate[b], Hidehiko Saito[a,1], George Stamatoyannopoulos[c], Tomoki Naoe[a]

[a]*Department of Hematology, Nagoya University Graduate School of Medicine, Tsurumai-cho 65, Showa-ku, Nagoya, 466-8550, Japan*
[b]*Nagoya University School of Health Sciences, Daiko-minami, 1-1-20, Higashi-ku, Nagoya, 461-8673, Japan*
[c]*Division of Medical Genetics, University of Washington, Seattle, WA, 98195-7720, USA*

Received 5 May 2004; received in revised form 15 December 2004; accepted 20 December 2004
Available online 6 January 2005

Abstract

FKLF-2 (KLF13) was cloned from fetal globin-expressing tissues and has been shown to be abundantly expressed in erythroid cells. In this study we examined the transcriptional regulation of the *KLF13* gene. A 5.5 kb 5′ flanking region cloned from mouse erythroleukemia (MEL) cell genomic DNA showed that major *cis* regulatory activities exist in the 550 bp sequence to the unique transcription start site, and that the promoter is more active in K562 cells than in COS-7 cells. The promoter was *trans*-activated by co-expressed GATA-1 through the sequence containing two CCAAT motifs, suggesting that GATA-1 is involved in the abundant expression of KLF13 mRNA in the erythroid tissue. Dual action, i.e. activating effect in COS-7 and repressive effect in K562 cell, was observed on its own promoter, suggesting a feedback mechanism for the transcriptional control of the KLF13 gene in the erythroid environment. These findings provide an insight on the mechanism of inducible mRNA expression of the *KLF13* gene in erythroid cells.

Keywords: Erythroid differentiation; KLF family; Promoter; Transcriptional regulation

1. Introduction

Proteins containing three contiguous Cys_2–His_2 zinc fingers similar to Sp1 or EKLF constitute a KLF family [1–3]. By using the zinc finger motif, these proteins bind to G-rich (GC or GT/CACCC) motifs that are widely distributed in *cis*-regulatory DNA sequences for gene expression. Some KLFs are ubiquitously expressed, while others show a tissue-restricted expression pattern. It may be reasonable to speculate that the non-ubiquitous KLFs are involved in cell type specific gene expression. Confirming this notion, EKLF (KLF1), which is specifically expressed in erythroid cells [4], plays a critical role for the expression of the β-globin gene [5,6] by interacting with the proximal CACCC motif of the β gene promoter [7,8]. LKLF (KLF2), which is predominantly expressed in the lung [9], is essential for the normal lung development since $LKLF^{-/-}$ ES cells do not contribute to the lung formation in chimeric mice [10]. KLFs thus play a substantial role in their major expression tissues.

Fetal *Krüppel*-like factor-2 (FKLF-2: KLF13) was originally cloned from mouse yolk sac and human fetal liver erythroid cells, i.e. fetal globin-expressing tissues [11]. It is predominantly expressed in the bone marrow, striated muscles and a subset of T cells. Other groups, in fact, cloned the same gene from these tissues [12,13]. Of note is that the mRNA expression of KLF13 gene is up-regulated upon the induction of differentiation with chemicals in cell lines with erythroid features [11]. Similarly, the expression of KLF13 protein is up-regulated upon the maturation of T cells [12]. These facts strongly suggest that KLF13 may be involved in the differentiation of the cells in which it is expressed. In addition KLF13 is a powerful activator of a broad range of promoters of erythroid genes in vitro [11]. These results suggest that

* Corresponding author. Tel.: +81 52 744 2158; fax: +81 52 744 2141.
E-mail address: asanoh@med.nagoya-u.ac.jp (H. Asano).
[1] Present address: Nagoya National Hospital, Sannomaru 4-1-1, Naka-ku, Nagoya 460-0001, Japan.

0167-4781/$ - see front matter © 2004 Elsevier B.V. All rights reserved.
doi:10.1016/j.bbaexp.2004.12.007

KLF13 plays a role in the development of erythroid phenotype. The transcriptional regulation for KLF13 gene expression may therefore be a part of molecular events of erythroid cell differentiation.

In this study we have cloned the 5′ flanking region of the mouse KLF13 gene. The promoter activity of the DNA fragment was tested in both erythroid (K562) and non-erythroid (COS-7) cells. Our data show that: the KLF13 gene promoter is more active in the erythroid environment than in the non-erythroid environment; and GATA-1 and KLF13 itself may have substantial effect in the transcriptional regulation of the KLF13 gene expression.

2. Materials and methods

2.1. Isolation of 5′ flanking DNA of the KLF13 gene

The 5′ flanking region of *KLF13* gene was obtained by inverse PCR (Fig. 1A). Four hundred nanograms of genomic

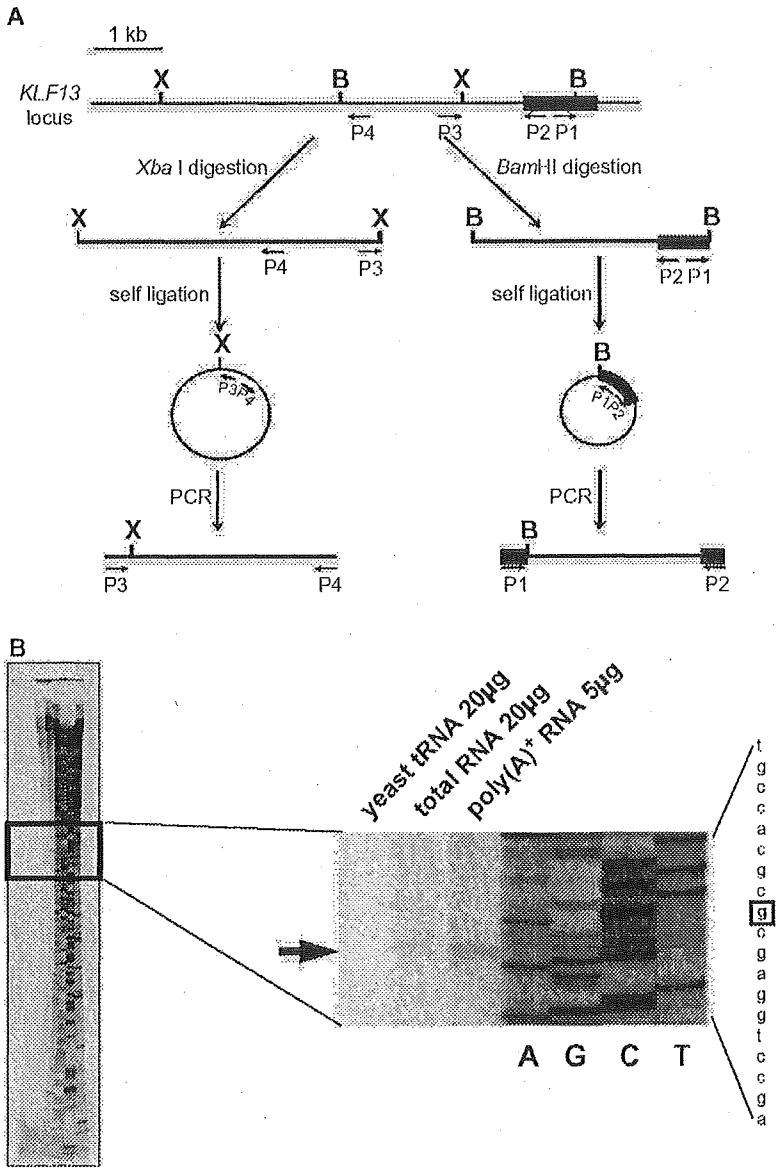

Fig. 1. Promoter of the *KLF13* gene. (A) Cloning of the 5′ flanking region of *KLF13* gene by inverse PCRs. The first exon is shown by a solid rectangle. B and X represent the *Bam*HI and *Xba*I sites, respectively. Primers used in inverse PCRs are indicated by arrows (P1–P4). Note that the positions of upstream *Bam*HI and *Xba*I sites are unknown prior to the experiments. (B) Primer extension analysis of KLF13 mRNA. RNAs used in the analysis are indicated above. Products of the sequencing reaction using the same probe were run on gel together, of which reading is shown at right. An arrow indicates the position of the extension product. The nucleotide in the sequence is highlighted by a square.